CHEMISTRY
A EUROPEAN JOURNAL

DOI: 10.1002/chem.200802128

Lactide Polymerisation with Air-Stable and Highly Active Zinc Complexes with Guanidine–Pyridine Hybrid Ligands

Janna Börner,[a] Ulrich Flörke,[a] Klaus Huber,[b] Artjom Döring,[c] Dirk Kuckling,[c] and Sonja Herres-Pawlis*[a]

Abstract: The synthesis of zinc complexes of guanidine–pyridine hybrid ligands [Zn(DMEGpy)Cl_2] (**C1**), [Zn(TMGpy)Cl_2] (**C2**), [Zn(DMEGqu)Cl_2] (**C3**), [Zn(TMGqu)Cl_2] (**C4**), [Zn(DMEGpy)$(CH_3COO)_2$] (**C5**), [Zn(TMGpy)$(CH_3COO)_2$] (**C6**), [Zn(DMEGqu)$(CH_3COO)_2$] (**C7**), [Zn(TMGqu)$(CH_3COO)_2$] (**C8**), [Zn(DMEGqu)$_2(CF_3SO_3)$][CF_3SO_3] (**C9**) and [Zn(TMGqu)$_2(CF_3SO_3)$][CF_3SO_3] (**C10**) is reported. These zinc complexes were completely characterised and screened regarding their activity in the ring-opening polymerisation of D,L-lactide. They proved to be active initiators in lactide bulk polymerisation, and polylactides with molecular weights (M_w) up to 176000 g mol^{-1} could be obtained. They combine high activity with robustness towards moisture and air. The influence of reaction temperature and of the anionic component of the zinc salt on the activity of the catalyst, as well as the occurrence of undesired side reactions, was investigated. By correlating these findings with the structural study on the zinc complexes we could deduce a structure–reactivity relationship for the zinc catalysts. This study was accompanied by DFT calculations. The bis-chelate triflate complexes **C9** and **C10**, supported by quinoline–guanidine ligands **L3** and **L4**, exhibit by far the highest reactivity. Systematic comparison of these complexes with their mono-chelate counterparts and their bis-guanidine analogues allows the attributes that promote polymerisation by neutral guanidine ligand systems to be elucidated: accessibility to the zinc centre and Lewis acidity.

Keywords: biodegradable polymers · density functional calculations · N ligands · ring-opening polymerisation · sustainable chemistry · zinc

Introduction

Over the past few decades biodegradable polymers have attracted increasing interest in fundamental research and in the chemical industry. Polylactides (PLA) have proven to be the most attractive and useful class of biodegradable polyesters among the numerous polyesters studied so far. Due to their favourable and sustainable material properties, as well as their broad range of applications reaching from packaging (bottles, films), fibres for tissue and clothes, to use in medical and pharmaceutical fields (retarding drugs, biodegradable screws and sutures) and the fact that they can be produced from inexpensive renewable raw materials like corn, sugar beets or even agricultural waste, PLAs are qualified to be a viable alternative to petrochemical-based plastics. To achieve high molecular weight, PLAs are obtained by metal-catalysed ring-opening polymerisation (ROP) of lactide, the cyclic diester of lactic acid (Scheme 1).[1–10]

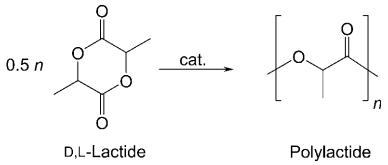

Scheme 1. ROP of D,L-lactide.

[a] M. Sc. J. Börner, Dr. U. Flörke, Dr. S. Herres-Pawlis
Department Chemie, Anorganische Chemie
Universität Paderborn
Warburger Straße 100, 33098 Paderborn (Germany)
Fax: (+49) 5251-603423
E-mail: shp@mail.uni-paderborn.de

[b] Prof. Dr. K. Huber
Department Chemie, Physikalische Chemie
Universität Paderborn
Warburger Straße 100, 33098 Paderborn (Germany)

[c] Dipl.-Chem. A. Döring, Prof. Dr. D. Kuckling
Department Chemie, Organische Chemie
Universität Paderborn
Warburger Straße 100, 33098 Paderborn (Germany)

Supporting information for this article is available on the WWW under http://dx.doi.org/10.1002/chem.200802128.

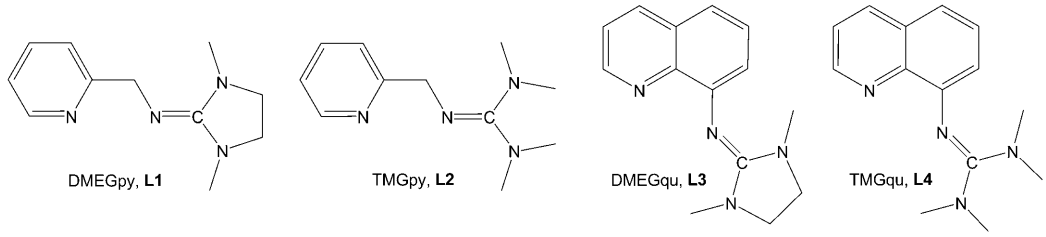

Scheme 2. Guanidine–pyridine hybrid ligands.[26]

Today, PLA is produced by more than ten chemical companies worldwide and has already left the niche of exotic polymers. For industrial production the most widely used initiator is tin(II) ethylhexanoate ($SnOct_2$), but the fact that all tin compounds are cytotoxic[1,11] is forcing the development of alternative initiators, especially when PLAs are intended for pharmaceutical, medical or food applications. Non-toxic options are zinc salts or complexes.[1] Because they are mostly colourless, inexpensive and non-toxic[2,3] zinc complexes with N-donor-functionalised ligands, for instance, β-diketiminates[12,13] and Schiff bases,[14] were introduced as active catalysts for the ROP of lactide to enhance the polymerisation process and to replace the common Sn-based catalysts. Besides the cationic portion, the influence of the anionic component is important as well.[15] In spite of great efforts in this field, there is still demand for highly active, non-toxic and stable complexes which can be easily handled.[16]

As we reported recently,[17] zinc guanidine complexes combine great potential as active catalysts in the ROP of D,L-lactide with acceptable stability. Several examples of zinc guanidine complexes have already been reported,[18] whereof some complexes have catalytic activity in selected processes, which makes guanidines a very promising ligand class leading to catalytically active zinc complexes.[19] The anionic guanidinate ligands have already been shown to stabilise lactide-polymerising complexes, but they are sensitive to moisture and air.[20,21] A related ligand class is represented by the 2-iminoimidazolines[22] which offer good donor properties and stabilise catalytically active complexes as well.[23]

To improve the activity of guanidine-based zinc complexes we modified the ligand system by substituting one guanidine moiety by an amine group. This changes the electronic environment by replacing one "hard" guanidine function by a "soft" pyridine donor and simultaneously increases accessibility to the zinc centre by substituting one bulky guanidine by a non-bulky pyridine unit. These guanidine–amine hybrid ligands combine the excellent donor properties of guanidines with additional coordination space for pre-coordination of substrates, and their modular synthesis protocol, which combines different spacer and guanidine groups, permits flexible ligand design.[24,25] The use of pyridyl and quinolyl units leads to the guanidine–pyridine hybrid ligands *N*-(1,3-dimethylimidazolidin-2-yliden)pyridin-8-amine (DMEGpy, **L1**), 1,1,3,3-tetramethyl-2-[(pyridin-2-yl)methyl]-guanidine (TMGpy, **L2**), *N*-(1,3-dimethylimidazolidin-2-yliden)quinolin-8-amine (DMEGqu, **L3**) and 1,1,3,3-tetramethyl-2-(quinolin-8-yl)guanidine (TMGqu, **L4**), which are depicted in Scheme 2.[26]

Herein we report on the synthesis and characterisation of the first zinc complexes of guanidine–pyridine hybrid ligands DMEGpy (**L1**), TMGpy (**L2**), DMEGqu (**L3**) and TMGqu (**L4**). These zinc complexes were screened for their catalytic activities in the polymerisation of lactide. The study extensively correlates experimental results with DFT calculations to rationalise the reactivity. Furthermore, we show that the classical conflict between stability and activity can be compensated by an integrated approach.

Results and Discussion

Synthesis of the zinc complexes: Guanidine–pyridine hybrid ligands **L1**–**L4** were synthesised by condensation of *N*,*N*′-dimethylethylenechloroformamidinium chloride (DMEG) and *N*,*N*,*N*′,*N*′-tetramethylchloroformamidinium chloride (TMG) (analogues of Vilsmeier salts) with 2-picolylamine and 8-aminoquinoline in high yields of up to 98%.[26] Their reaction with zinc salts ($ZnCl_2$, $Zn(CH_3COO)_2$, $Zn(CF_3SO_3)_2$) in a dry, aprotic solvent (MeCN, THF) resulted in straightforward formation of zinc complexes **C1**–**C10** (see Table 1). They could be isolated as colourless (**C1**, **C2**, **C5**, **C6**) or yellow crystals (**C3**, **C4**, **C7**–**C10**) in yields of 64–99%.

Table 1. Overview of the synthesised zinc complexes of guanidine–pyridine hybrid ligands.

	$ZnCl_2$	$Zn(CH_3COO)_2$	$Zn(CF_3SO_3)_2$
DMEGpy (**L1**)	[Zn(DMEGpy)Cl_2] (**C1**)	[Zn(DMEGpy)$(CH_3COO)_2$] (**C5**)	–[a]
TMGpy (**L2**)	[Zn(TMGpy)Cl_2] (**C2**)	[Zn(TMGpy)$(CH_3COO)_2$] (**C6**)	–[a]
DMEGqu (**L3**)	[Zn(DMEGqu)Cl_2] (**C3**)	[Zn(DMEGqu)$(CH_3COO)_2$] (**C7**)	[Zn(DMEGqu)$_2$$(CF_3SO_3)$][$CF_3SO_3$] (**C9**)
TMGqu (**L4**)	[Zn(TMGqu)Cl_2] (**C4**)	[Zn(TMGqu)$(CH_3COO)_2$] (**C8**)	[Zn(TMGqu)$_2$$(CF_3SO_3)$][$CF_3SO_3$] (**C10**)

[a] These complexes could not be structurally characterised.

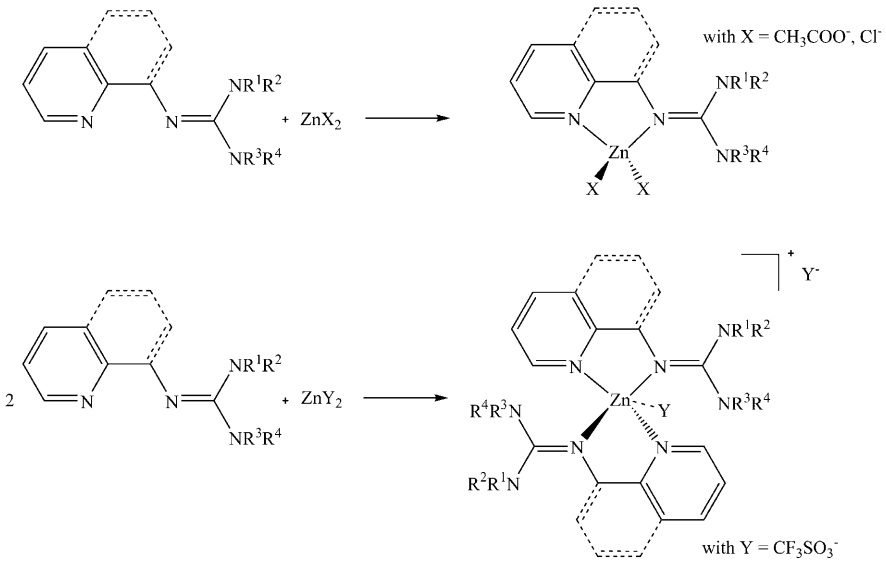

Scheme 3. General complex synthesis.

Single crystals of the complexes were obtained either by cooling a saturated solution slowly to room temperature or by slow diffusion of diethyl ether into the solution. The resulting crystals have high stability towards moisture and air. They can be handled and stored in air, whereas the corresponding guanidine–pyridine hybrid ligands and zinc salts are sensitive towards hydrolysis or rather hygroscopic.

The molecular structures of **C1**–**C10** (Figures 1–6 and Figures S1–S4 in the Supporting Information) were determined by X-ray crystallography. In the complexes with zinc chloride and zinc acetate, the zinc atom is fourfold coordinated by the two N-donor atoms of the guanidine–pyridine hybrid ligands and two chlorine ions or two acetate ions, respectively. However, in the complexes with zinc triflate, the zinc atom is fourfold coordinated by two chelate ligands (Scheme 3). The above-described zinc complexes formed independently of the molar ratio of the starting materials.

Due to their structural similarity the groups of complexes containing zinc chloride, zinc acetate and zinc triflate will be discussed in groups.

Complexes with zinc chloride: The structures of the zinc chloride complexes [Zn(DMEGpy)Cl_2] (**C1**), [Zn(TMGpy)Cl_2] (**C2**), [Zn(DMEGqu)Cl_2] (**C3**) and [Zn(TMGqu)Cl_2] (**C4**) are very similar to each other (Figures 1 and 2 and Figures S1 and S2 in the Supporting Information). Selected bond lengths and angles of the compounds are collected in Table 2.

In all complexes each zinc atom is fourfold coordinated, whereby two coordination sites are occupied in a chelating manner by the N-donor atoms of the guanidine–pyridine hybrid ligands to form a five-membered heterocycle. The two Zn–Cl bonds in **C1** are equal in length (av 2.240 Å), but in **C2, C3** and **C4** one bond is longer than the other. In these complexes the longer Zn–Cl bond measures 2.236 Å (av) and the shorter one 2.215 Å (av). The distances between the zinc atom and the N-donor atoms of the guanidine–pyridine hybrid ligands differ due to the different coordination properties of the N-donor atoms. In **C1**, **C3** and **C4** the corresponding lengths are equal and amount to 2.045 Å (av) for $Zn–N_{py}$ and 2.036 Å (av) for $Zn–N_{gua}$, but in **C2** the $Zn–N_{py}$ bond is 0.02 Å (2.065(2) Å) longer and the $Zn–N_{gua}$ bond 0.27 Å (2.009(2) Å) shorter than the average values of the other complexes. The $C_{gua}–N_{gua}$ double bonds range in length from 1.317(1) to 1.335(2) Å and show the tendency of being slightly shorter for pyridine ligands. Remarkably, in all four complexes the ligands have the

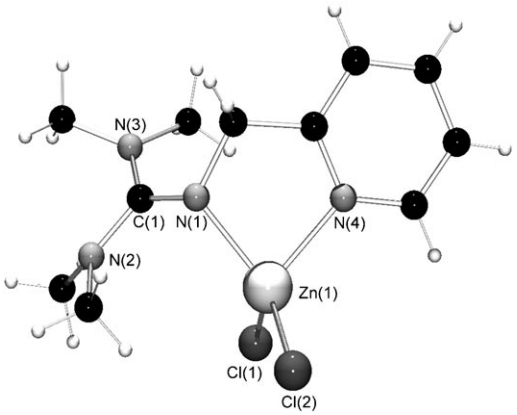

Figure 1. Molecular structure of [Zn(TMGpy)Cl_2] (**C2**) as determined at 153 K.

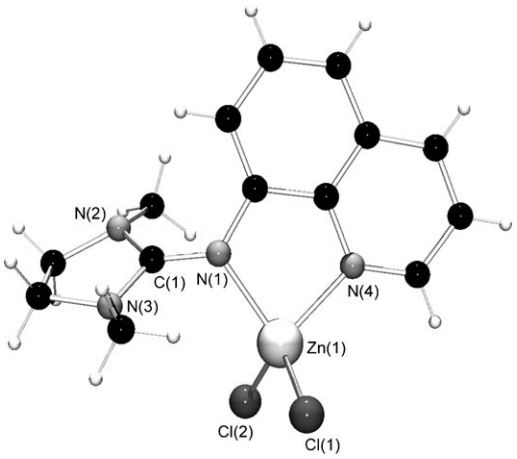

Figure 2. Molecular structure of [Zn(DMEGqu)Cl_2] (**C3**) as determined at 120 K.

Table 2. Selected bond lengths [Å] and angles [°] of **C1**–**C4**.

	C1	C2	C3	C4
$Zn-N_{py}$	2.047(1)	2.065(2)	2.045(1)	2.044(1)
$Zn-N_{gua}$	2.036(1)	2.009(2)	2.039(1)	2.034(1)
Zn–Cl	2.237(1)	2.215(1)	2.212(1)	2.217(1)
	2.243(1)	2.235(1)	2.234(1)	2.238(1)
$C_{gua}-N_{gua}$	1.317(2)	1.317(3)	1.327(2)	1.335(2)
$C_{gua}-N$	1.375(2)	1.356(3)	1.355(2)	1.347(2)
	1.362(2)	1.360(3)	1.352(2)	1.357(2)
N–Zn–N	83.74(5)	82.57(7)	82.56(5)	82.34(5)
$\sphericalangle(ZnCl_2, ZnN_2)$	83.40(3)	85.07(5)	84.39(3)	79.31(3)
$\sphericalangle(C_{gua}N_3, ZnN_2)$	18.92(4)	48.57(8)	53.38(6)	55.92(5)
$\sphericalangle(C_{gua}N_3, NC_3)$ (av)	9.8	33.7	12.6	29.5
ρ	0.96	0.97	0.98	0.99

same bite angle of 82.80° (av), which differs considerably from the tetrahedral angle (109.47°). This leads to a distorted tetrahedral coordination geometry of the zinc atom. This is also reflected in the dihedral angle between the $ZnCl_2$ and ZnN_2 planes. In ideal tetrahedral coordination geometry it is 90°, but in the present complexes these angles are 83.40(3) (**C1**), 85.07(5) (**C2**), 84.39(3) (**C3**) and 79.31(3)° (**C4**).

To evaluate the influence of the guanidine–pyridine hybrid ligands on the structure, complexes **C1**–**C4** were compared with the already reported bipyridine compounds [Zn(bipy)Cl_2] (bipy = 2,2′-bipyridine)[27] and [Zn(phen)Cl_2] (phen = 1,10-phenanthroline)[28] as well as the bis-guanidine complex [Zn($DMEG_2e$)Cl_2] ($DMEG_2e$ = N^1,N^2-bis(1,3-dimethylimidazolidin-2-ylidene)ethane-1,2-diamine).[17] The Zn–Cl bonds in the bipyridine complexes are of different length, as in **C2**, **C3** and **C4**. The longer ones ([Zn(bipy)Cl_2]: 2.210(1) Å, [Zn(phen)Cl_2]: 2.207(3) Å) conform to the shorter bond of **C2**, **C3** and **C4**, whereas the short ones are 0.017 Å shorter [Zn(bipy)Cl_2]: 2.198(1) Å, [Zn(phen)Cl_2]: 2.198(3) Å]. The Zn–Cl bonds in the bis-guanidine complex are equal, and with values of 2.260(1) Å they are longer than those in all the other complexes. The $Zn-N_{gua}$ distances of [Zn($DMEG_2e$)Cl_2] (2.038(2) Å) correspond to those in **C1**, **C3** and **C4**, and the $Zn-N_{py}$ bond lengths in [Zn(bipy)Cl_2] (2.064(2), 2.053(2) Å) and [Zn(phen)Cl_2] (2.072(7) and 2.050(7) Å) to those of **C1**–**C4**. The bite angles of the bipyridine ligands are slightly smaller ([Zn(bipy)Cl_2]: 80.3(1)°, [Zn(phen)Cl_2]: 80.4(3)°), and the bite angle of the guanidine ligand ([Zn($DMEG_2e$)Cl_2]: 86.18(10)° slightly widened. The $C_{gua}-N_{gua}$ bond length of the bis-guanidine complex of 1.309(3) Å is smaller than the average length of the corresponding bond in the complexes **C1**–**C4**.

Complexes with zinc acetate: The molecular structures of [Zn(DMEGpy)($CH_3COO)_2$] (**C5**), [Zn(TMGpy)($CH_3COO)_2$] (**C6**), [Zn(DMEGqu)($CH_3COO)_2$] (**C7**) and [Zn(TMGqu)($CH_3COO)_2$] (**C8**), obtained by reaction of zinc acetate with **L1**–**L4**, are shown in Figures 3, 4 and the Supporting Information (Figure S3 and S4), and Table 3 lists selected bond lengths and angles. The crystal of **C5** contains

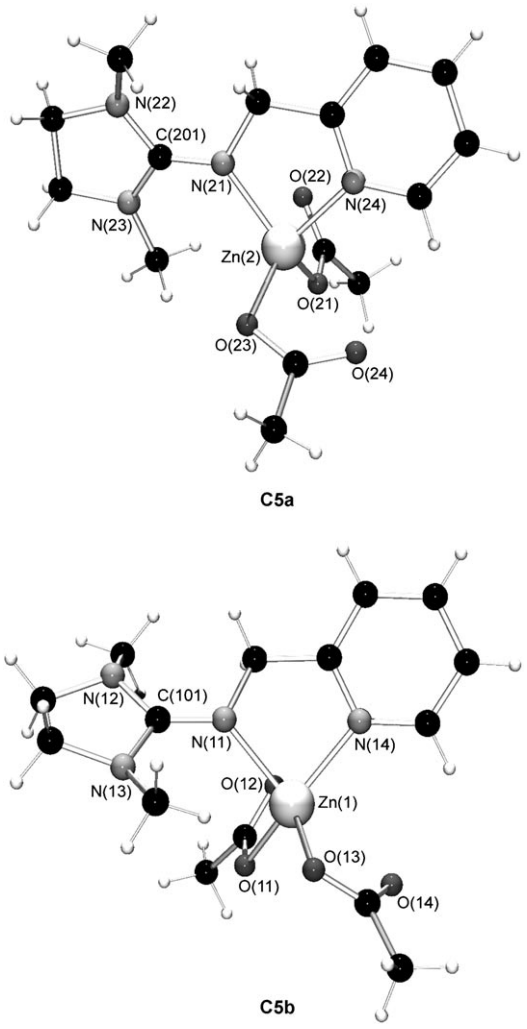

Figure 3. Molecular structures of [Zn(DMEGpy)($CH_3COO)_2$] (**C5a** and **C5b**) as determined at 120 K.

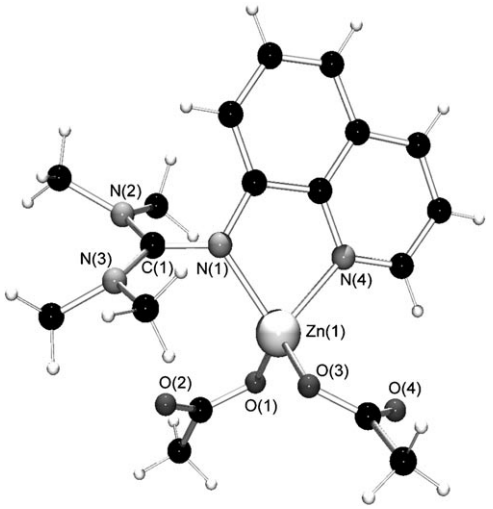

Figure 4. Molecular structure of [Zn(TMGqu)($CH_3COO)_2$] (**C8**) as determined at 120 K.

Table 3. Selected bond lengths [Å] and angles [°] of **C5**–**C8**.

	C5a	C5b	C6	C7	C8
Zn–N_{py}	2.036(2)	2.058(2)	2.062(2)	2.048(1)	2.080(1)
Zn–N_{gua}	2.038(2)	2.075(2)	2.044(2)	2.106(1)	2.054(1)
Zn–O	1.946(1)	1.952(1)	1.934(2)	1.950(1)	1.951(1)
	1.952(1)	2.005(1)	1.978(2)	2.021(1)	1.958(1)
C_{gua}–N_{gua}	1.313(2)	1.310(2)	1.321(4)	1.336(2)	1.344(2)
C_{gua}–N	1.367(2)	1.375(2)	1.365(4)	1.336(2)	1.343(2)
	1.348(2)	1.368(2)	1.358(4)	1.364(2)	1.348(2)
N–Zn–N	83.57(6)	81.82(6)	82.68(10)	80.94(5)	81.33(5)
∢(ZnO_2, ZnN_2)	76.32(6)	73.13(6)	82.8(1)	78.40(5)	85.83(5)
∢($C_{gua}N_3$, ZnN_2)	14.3(1)	40.96(6)	43.0(1)	48.14(7)	55.44(6)
∢($C_{gua}N_3$, NC_3) (av)	9.4	15.5	33.3	11.3	27.1
ρ	0.97	0.96	0.97	0.99	1.00

two crystallographically independent molecules per asymmetric unit with the same molecular composition but different structural properties, denoted by **C5a** and **C5b**.

The zinc atoms of all complexes are fourfold coordinated by the N-donor atoms of the guanidine–pyridine hybrid ligands and by the oxygen atoms of two acetate ions. The coordination geometry of the zinc centre can be best described as a distorted tetrahedron. The bite angles of the coordinated ligands, which range from 80.94 to 83.57°, are notably smaller than the tetrahedral angle. The distorted geometry is also reflected in the dihedral angles between the ZnO_2 and ZnN_2 planes, which exhibit on average a deviation of 11° from the ideal tetrahedral arrangement. In **C5a** and **C8** the two Zn–O bond lengths are equal (av 1.949 and 1.955 Å), whereas the other complexes contain one shorter (**C5b**: 1.952(1); **C6**: (1.934(2); **C7**: 1.950(1) Å) and one longer bond (**C5b**: 2.005(1); **C6**: 1.978(2); **C7**: 2.021(1) Å). The Zn–N bonds show no apparent influence of the kind of N-donor, as was found for the chlorido complexes. In **C5a** the two bond lengths are equal (av 2.037 Å). In the complexes with a DMEG guanidine unit the Zn–N_{gua} bond is longer than the Zn–N_{py} bond, whereas in those with a TMG guanidine unit the Zn–N_{gua} bond is shorter than the Zn–N_{py} bond. The C_{gua}=N_{gua} double bond lengths range from 1.310(2) to 1.344(2) Å. By trend the C_{gua}=N_{gua} bonds in the quinoline ligands are apparently 0.02 Å longer than those in the pyridine ligands.

Complexes **C5**–**C8** can be compared with the already reported bipyridyl complex [Zn_2(1,1,2,2-tetrakis(2-pyridyl)-ethane)$(CH_3COO)_4$][29] and the bis-guanidine complex diaceta-to[N^1,N^2-bis(1,3-dimethylimidazolidin-2-ylidene)ethane-1,2-diamine]zinc(II)[17] to quantify the influence of the guanidine–pyridine hybrid ligands on the structure of the complex. The Zn–O distances of the pyridyl complex (1.946(2), 1.974(2) Å) and the bis-guanidine complex (1.969(2), 1.956(2) Å) lie in the same range as those in **C5**–**C8**. One Zn–N_{py} bond of the pyridyl complex (2.119(2) Å) is slightly longer than the average bond length of the zinc acetato complexes stabilised by guanidine–pyridine hybrid ligands, whereas the other (2.094(2) Å) lies in the same range. One of the Zn–N_{gua} bonds in the bis-guanidine complex (2.011(2) Å) is slightly shorter than the average in **C5**–**C8**, whereas the other (2.038(2) Å) fits well to the average. The C_{gua}–N_{gua} bonds do not differ much (1.308(2), 1.305(2) Å).

All tetrahedrally coordinated zinc complexes with guanidine–pyridine hybrid ligands show twisting of the guanidine plane (CN_3) with respect to the coordination plane (N-Zn-N) to avoid steric interactions. The dihedral angles increase with increasing steric demand of the guanidine–pyridine hybrid ligand in the order DMEGpy→TMGpy→DMEGqu→TMGqu. Complex **C5b** also fits the trend, although it differs by about 27° from **C5a**.

Complexes with zinc triflate: The molecular structures of zinc triflate complexes [Zn(DMEGqu)$_2$(CF_3SO_3)][CF_3SO_3] (**C9**) and [Zn(TMGqu)$_2$(CF_3SO_3)][CF_3SO_3] (**C10**) exhibit a different coordination of the zinc atom to the complexes of zinc chloride and zinc acetate (Figures 5 and 6). Each Zn atom is sixfold coordinated, whereby four coordination sites are occupied in a bis-chelating manner by the N-donor atoms of two guanidine–pyridine hybrid ligands. The remaining coordination sites are occupied by two oxygen atoms of one triflate anion, while the other triflate anion is far away from the complex centre and acts as counterion. The asymmetric unit contains Λ and Δ isomers of the complex cation of **C10**; thus, in the following only one structure

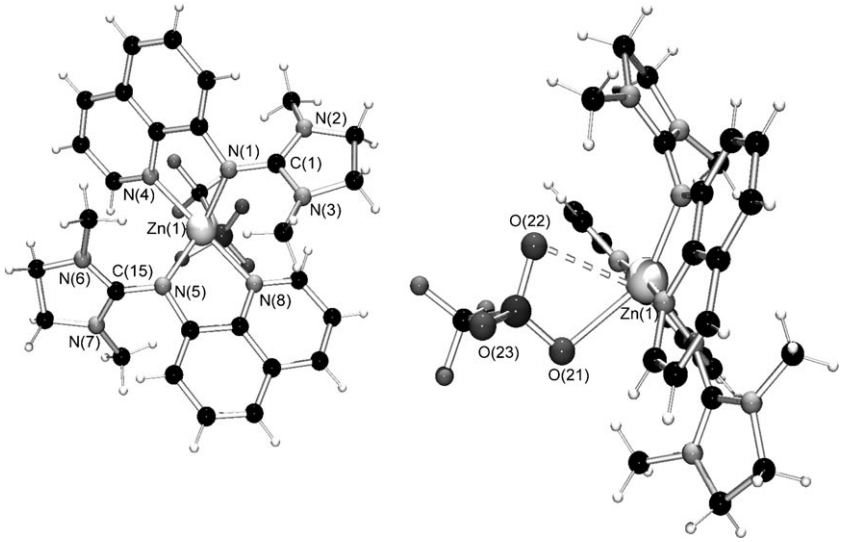

Figure 5. Molecular structure of [Zn(DMEGqu)$_2$(CF_3SO_3)]$^+$ in crystals of [Zn(DMEGqu)$_2$(CF_3SO_3)][CF_3SO_3] (**C9**) as determined at 120 K, depicted from two different directions.

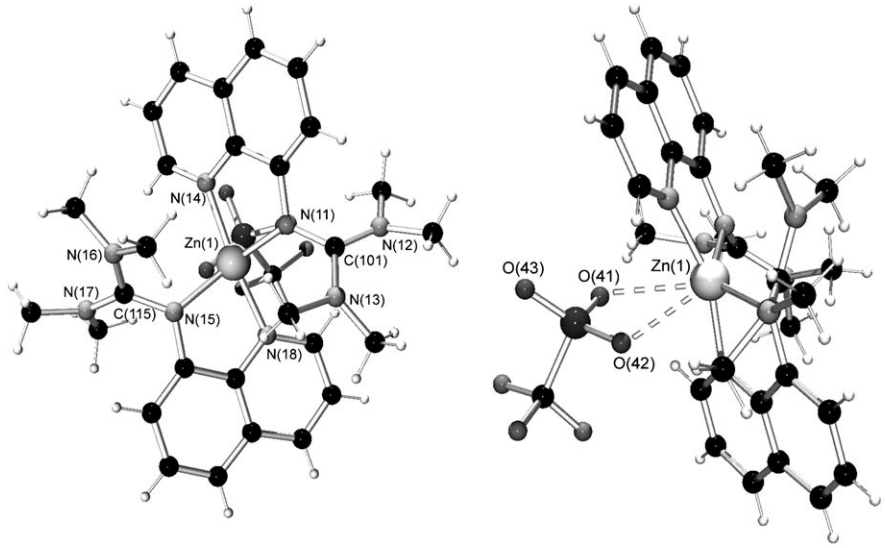

Figure 6. Molecular structure of $[Zn(TMGqu)_2(CF_3SO_3)]^+$ in crystals of $[Zn(TMGqu)_2(CF_3SO_3)][CF_3SO_3]$ (**C10**) as determined at 120 K. The Λ isomer is depicted from two different directions.

is discussed as **C10**. Selected bond lengths and angles of the compounds are collected in Table 4.

Table 4. Selected bond lengths [Å] and angles [°] of **C9** and **C10**.

	C9	**C10**
$Zn–N_{py}$	2.089(3)	2.052(3)
	2.091(3)	2.071(3)
$Zn–N_{gua}$	2.035(3)	2.031(3)
	2.049(3)	2.011(3)
Zn–O	2.452(7)	2.684(3)
	2.700(7)	2.698(3)
$C_{gua}–N_{gua}$	1.345(5)	1.357(5)
	1.340(5)	1.342(5)
$C_{gua}–N$	1.344(5), 1.337(5)	1.329(5), 1.352(5)
	1.340(5), 1.343(5)	1.344(5), 1.338(5)
N–Zn–N	81.4(1)	82.1(1)
	80.5 (1)	81.9(1)
$N_{py}–Zn–N_{py}$	172.0(1)	161.3(1)
$N_{gua}–Zn–N_{gua}$	122.3(1)	128.0(1)
$\measuredangle(ZnN_2, ZnN_2)$	60.6(1)	58.9(1)
$\measuredangle(C_{gua}N_3, ZnN_2)$	55.0(2), 59.4(1)	56.0(1), 52.9(2)
$\measuredangle(C_{gua}N_3, NC_3)$ (av)	9.0	28.0
ρ	1.00	1.01

The distances between the zinc atom and the pyridine donor atom are identical in each complex cation (**C9**: av 2.090; **C10**: av 2.062 Å) and significantly longer than the corresponding $Zn–N_{gua}$ bond lengths (**C9**: av 2.042; **C10**: av 2.021 Å). The $C_{gua}=N_{gua}$ bonds are also identical and exhibit an average value of 1.346 Å. The distances between the zinc and oxygen atoms in **C10** (2.684(3) and 2.698(3) Å) are very long but smaller than the sum of the van der Waals radii of 2.79 Å. The cationic complex unit of **C9** exhibits one short (2.452(7) Å) and one long Zn–O bond (2.700(7) Å). These long bonds indicate weak coordination, which is a prerequisite for coordination of a lactide molecule. The coordination geometry of the zinc centre can be best described as a distorted trigonal bipyramid in which the apical positions are occupied by the pyridine nitrogen atoms of the ligands. The equatorial sites are occupied by the guanidine nitrogen donors and the oxygen atoms of the triflate anion, which act as one equatorial donor. The metal atom lies in the trigonal plane in both complexes.

The fact that the N atoms of the two aromatic systems reside in the apical positions is in accordance with the properties of the two types of N atoms. Guanidine ligands have stronger σ-donating properties than pyridine ligands, and this leads to a decrease in the $Zn–N_{gua}$ bond length (bond to an equatorial side). The distortion of the coordination geometry is reflected in the angle between two axial sites: In trigonal-bipyramidal coordination the angle is 180°, but it is diminished to 172.0(1)° in **C9** and to 161.1(1)° in **C10**. The angle between the two nitrogen atoms in equatorial position (**C9**: 122.3(1)°, **C10**: 128.0(1)°) is near to the undistorted angle (120°). However, the angle between an equatorial and an axial site differs from the ideal value (90°) because of the fixed value for the bite angle (av 81.50°) and leads to another slight distortion. This distortion minimises the interactions between the sterically demanding guanidine residues and the aromatic parts. The structural motif of a trigonal bipyramid was already described for a cobalt complex of the ligand DMEGqu (**L3**).[26] A further effect is torsion of the $ZnN_{2,ligand}$ and $ZnN_{2,ligand'}$ plane by 60.6(1)° in **C9** and 58.9(1)° in **C10** with respect to each other. The angles between the $C_{gua}N_3$ and ZnN_2 planes in **C9** (55.0(2) and 59.4(1)°) are similar to those in **C10** (56.0(1) and 52.9(2)°), because in both complexes the metal centre is comparably crowded and the steric interactions should be reduced.

Structural influence of the guanidine unit: In all reported zinc complexes with guanidine–pyridine hybrid ligands twisting within the guanidine moiety can be observed which is characteristic for peralkylated guanidine units.[24,26] This twisting is a result of the interplay between the electronic effect of the intraguanidine conjugation (driving towards planarity) and the evasion of the alkyl substituents.

The average angle between the $C_{gua}N_3$ and NC_3 plane is 30.3° for TMG and 11.3° for DMEG. Twisting within TMG is more distinct because of the free rotation of the methyl groups connected to the amine function, whereas in DMEG twisting is hindered by the rigid ethylene bridge between the amine groups of the guanidine moiety.

Delocalisation of the positive charge within the guanidine unit and the resultant levelling of the C–N bond lengths can be expressed by the structural parameter ρ (see Scheme 4).[30] A ρ value of 1 means complete delocalisation

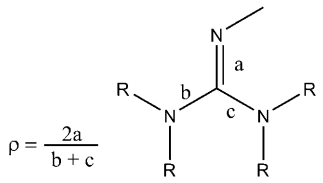

Scheme 4. Calculation of the structural parameter ρ.

of the positive charge and total bond levelling. The ρ values of the chlorido complexes increase from **C1** (0.96), **C2** (0.97), **C3** (0.98) to **C4** (0.99). The general trend that delocalisation in complexes with quinoline ligands is higher than in those with pyridine ligands is also found for the acetato complexes. The ρ values for the corresponding pyridine complexes are 0.96 (**C5b**) and 0.97 (**C5a**, **C6**), whereas those of the quinoline complexes of 0.99 (**C7**) and 1.00 (**C8**) are considerably higher. Besides this trend in the structural parameter ρ, the C=N bonds in quinoline containing complexes are about 0.02 Å longer than those in the pyridine-containing complexes. The bis-chelate complexes **C9** and **C10** show complete delocalisation of the positive charge in the guanidine unit. Altogether these complexes show a high degree of delocalisation.

We have found a correlation between the twisting of the guanidine unit with respect to the chelate plane and the levelling of the C–N bonds. Interestingly, the only exception is **C5b**. The more the guanidine unit twists out of the chelate plane to minimise the disadvantageous interaction with sterically demanding groups, the higher the ρ value and the greater the delocalisation and bond levelling. A possible explanation is that the guanidine unit leaves the conjugation of the aromatic system (quinoline or pyridine) by twisting and acts as isolated donor.

DFT calculations: The structural trends described above were investigated by gas-phase DFT calculations. The electronic structures of zinc complexes **C1**–**C10** were examined by using B3LYP density functional theory and the 6-31G(d) and 6-31G+(d) basis sets, implemented in the Gaussian 03 suite of programs.[31] Geometry optimisations were performed by using the coordinates from X-ray data as starting point in case of **C1**–**C10**. The results of the optimisations are presented in Tables S1–S6 (see Supporting Information).

For the 6-31G(d) basis set, the computed structures of the complexes are in good agreement with their solid-state structures, whereas the 6-31G+(d) basis set generally yields too long bond lengths. The soft donating character of pyridine and guanidine units is significantly overestimated by this diffuse basis set, as has been observed in several cases.[32] For most complexes, the predicted Zn–N distances are about 0.03 Å too long, which is a known tendency for such systems.[32,33] Hence, ligands **L1**–**L4** and the model ligand HGqu were examined with B3LYP density functional theory and only the 6-31G(d) basis set (Table S6 in the Supporting Information and Figure 7).

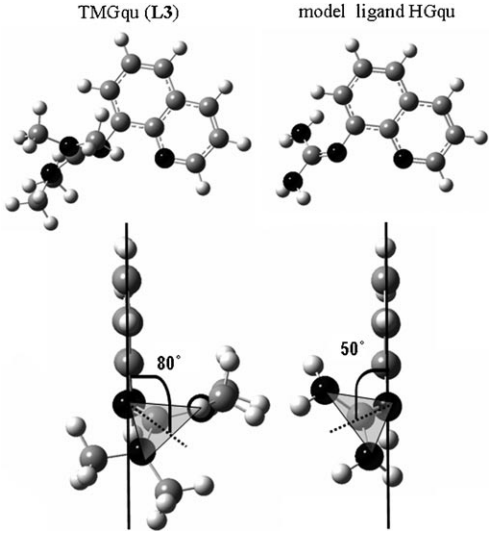

Figure 7. Comparison of the calculated structure of TMGqu (**L3**) with model ligand HGqu [RB3LYP/6-31G(d))]

The tetrahedral coordination environments in **C1**–**C8** are correctly described by both basis sets. Special emphasis is placed on the angles between the ZnN_2 and the ZnX_2 planes, which are in good accordance with those found in the solid state. The coordination of the acetate ions in the complexes **C5**–**C8** is in good agreement as well. Interestingly, for the acetato complexes, contacts of the benzyl or quinoline spacer hydrogen atoms to the acetate oxygen atoms are found, which were confirmed by DPFGSE-NOE NMR measurements in solution. For acetato complex **C5**, two conformers were found in the solid state. Their differences in $Zn–N_{py}$ and $Zn–N_{gua}$ bond lengths are reflected qualitatively in the DFT calculations, too. Their calculated energy difference of 1.4 kcal mol^{-1} explains their coexistence in the single crystal.

The bis-chelate complexes **C9** and **C10** are correctly described as well: the trigonal-bipyramidal coordination is well reflected in the N_{py}-Zn-N_{py} angles (169.5 for **C9** and 167.8° for **C10**) which describe the apical sites. Moreover, the η^2 binding mode of the triflate anion and the Zn–O bond lengths are in good agreement with the X-ray structures.

In comparison with the solid-state structures, the calculated C=N guanidine "double-bond" lengths are extremely close to the X-ray data. Especially the differences between the four coordinating ligands are well reflected: for TMGqu and DMEGqu complexes this bond is generally about 1.335 Å long, whereas for TMGpy and DMEGpy complexes it is shortened to about 1.317 Å. Concomitantly, the tendency for the structural parameter ρ is correctly predicted: the quinoline-containing systems exhibit a slightly higher ρ

(0.98–0.99) than the pyridine systems (0.94–0.96), which is in good accordance with the solid-state structures.

Moreover, particularly the fact that the guanidine units twist with respect to the chelate plane in dependence on the ligand in complexes **C1**–**C8** could be reproduced by DFT calculations. The following trend could be deduced: quinoline systems exhibit a contact between the guanidine substituents and the *ortho* position. To avoid steric hindrance, the whole guanidine unit twists by 45° with respect to the chelate plane. Simultaneously, the levelling within the guanidine unit increases up to $\rho = 1$ because the guanidine moiety leaves conjugation with the aromatic system. In the pyridine systems, the spacer is more flexible and allows other ways of avoiding steric hindrance between guanidine substituents and the rest of the ligand molecule, which results in a smaller twist angle accompanied by a smaller ρ value. As the same trend was found experimentally, it can not be related to packing effects but to intrinsic forces within the complexes.

The DFT analysis of the ligands and a model ligand without substituents (HGqu) shows that the focus on the steric interactions is only one aspect of this twisting effect (Figure 7). Even without substituents, twisting of up to 50° occurs. The aromatic influence is crucial for the guanidine system: the analysis of the Mulliken charges of the ligands (Table 8) reveals that the guanidine N imine atom is significantly more negatively charged in quinoline ligands and complexes than in pyridine ones. Furthermore, the guanidine double bonds in the quinoline ligands are calculated to have a mean length of 1.287 Å (pyridine–guanidine ligands: 1.283 Å), which is longer than the values for reported aliphatic guanidines (1.277 Å)[34] but in the range of aromatic guanidines (1.282 Å).[35] In aromatic guanidines, rotation around the C=N bonds is facilitated by the interaction with the aromatic system, which is manifested in coalescence behaviour for the corresponding guanidine substituents.[25] Thus, it is understandable that the C=N bonds are longer and the C–N bonds shorter than in the pyridine systems where the guanidine moiety is bound to the benzyl group and not directly to the aromatic ring. Hence, in the quinoline systems the ρ value must be higher than in the pyridine systems for electronic reasons.

For a more detailed analysis of the electronic structure the Mulliken charges were determined for the ligands and their complexes (Tables 5–8). These do not represent absolute charges but the trends among the complexes give an impression of electronic effects. A pronounced effect is the difference between the DMEG and TMG groups. As the geometry optimisations predict, the intra-guanidine twist is significantly smaller in the DMEG groups (12°) because of the ethylene backbone, which geometrically restricts intra-guanidine torsion. In all analysed complexes, the imine N atom in DMEG groups is around 0.05 more negatively charged than that in TMG groups. At the same time, the corresponding amine N atoms in the DMEG-containing systems are slightly more negatively charged, and the central guanidine C atoms are considerably more positively charged than those in the TMG-containing systems. This result is in good accordance with the theoretical calculations on TMG- and DMEG-containing ligands performed by Tamm et al.[23a]

An important result of this analysis is the remarkable positive charge on the zinc atom in the bis-chelate complexes of 1.004 (**C9**) and 0.994 (**C10**) in comparison to around 0.68 for the chlorido complexes and about 0.87 for the acetato complexes. This finding documents the higher Lewis acidity of the zinc atom in **C9** and **C10** compared to **C1**–**C8**.

NMR spectroscopy: Since we found twisting of the guanidine plane relative to the coordination plane in the solid

Table 5. Mulliken charges in electron units (charge of electron is equal to −1) of **C1**, **C2**, **C5** and **C6** (RB3LYP, 6-31G(d)).

	C1	**C2**	**C5a**	**C5b**	**C6**
Zn	0.682	0.667	0.860	0.872	0.862
N_{py}	−0.571	−0.566	−0.579	−0.598	−0.580
N_{gua}	−0.675	−0.622	−0.659	−0.673	−0.615
C_{gua}	0.823	0.696	0.796	0.811	0.680
N_{amine}	−0.458	−0.404	−0.449	−0.449	−0.422
	−0.475	−0.423	−0.469	−0.478	−0.405
X = Cl, OAc	−0.516	−0.494	−0.600	−0.608	−0.618
	−0.518	−0.530	−0.618	−0.612	−0.597

Table 6. Mulliken charges in electron units (charge of electron is equal to −1) of **C3**, **C4**, **C7** and **C8** (RB3LYP/6-31G(d)).

	C3	**C4**	**C7**	**C8**
Zn	0.692	0.697	0.881	0.886
N_{py}	−0.644	−0.641	−0.657	−0.650
N_{gua}	−0.781	−0.745	−0.788	−0.755
C_{gua}	0.806	0.684	0.812	0.706
N_{amine}	−0.451	−0.403	−0.434	−0.411
	−0.458	−0.409	−0.454	−0.392
X = Cl, OAc	−0.502	−0.501	−0.610	−0.606
	−0.536	−0.530	−0.602	−0.606

Table 7. Mulliken charges in electron units (charge of electron is equal to −1) of **C9** and **C10** (RB3LYP/6-31G(d)).

	C9	**C10**
Zn	1.004	0.994
N_{py}	−0.638, −0.641	−0.655, −0.619
N_{gua}	−0.811, −0.792	−0.736, −0.771
C_{gua}	0.800, 0.757	0.648, 0.645
N_{amine}	−0.447, −0.448	−0.399, −0.399
	−0.443, −0.448	−0.395, −0.392
O	−0.617	−0.601
	−0.621	−0.668

Table 8. Mulliken charges of ligands **L1**–**L4** (RB3LYP, 6-31G(d)).

	DMEGpy (**L1**)	TMGpy (**L2**)	DMEGqu (**L3**)	TMGqu (**L4**)
N_{py}	−0.473	−0.460	−0.501	−0.490
N_{gua}	−0.544	−0.469	−0.598	−0.525
C_{gua}	0.722	0.606	0.756	0.613
N_{amine}	−0.478	−0.417	−0.455	−0.419
	−0.454	−0.424	−0.461	−0.421

state and in the gas-phase DFT calculations we investigated the existence of a preferred configuration in solution. Temperature-dependent ^{1}H NMR spectra of complexes **C3**, **C4** and **C7–C10** and the free ligands **L3** and **L4** were measured to determine whether it is possible to stop rotation of the C=N bond. In the case of a frozen rotation, DPFGSE-NOE NMR spectra should determine whether there is a NOE contact between the hydrogen atom of the quinoline carbon atom in *ortho* position to the guanidine moiety and a hydrogen atom of the methyl groups of the guanidine unit. However, even at −90 °C the rotation of the C=N bond is still present, so no preferred configuration is ascertainable.

Polymerisation activity: We reported recently[17] that bis-guanidine zinc complexes have catalytic activity in the ring-opening polymerisation of D,L-lactide and offer the advantage of acceptable stability towards air and moisture. Thus, zinc complexes of guanidine–pyridine hybrid ligands **C1–C10** were investigated for their activity in bulk polymerisation of D,L-lactide. The ligand design strategy focuses on two points. First, improving accessibility to the zinc centre for the pre-coordination of substrates requires the substitution of one bulky guanidine by a non-bulky pyridine unit. Second, the electronic environment is modified by replacing one "hard" guanidine N-donor group by the "soft" N donor of the pyridine unit.

For the polymerisation procedure the monomer D,L-lactide and the zinc initiator (I/M ratio 1:500 or 1:1000) were heated at 130 or 150 °C. After a reaction time of 24 h or 48 h, the melt was dissolved in dichloromethane, and then the PLA was precipitated in cold ethanol, isolated and dried under vacuum at 50 °C. To rate the catalytic activity of the complexes, the polymer yield was determined, and the molecular weights and polydispersity of the obtained PLA were investigated by gel permeation chromatography (see Table 9). As reference experiments, the polymerisation activity of zinc salts, the pure ligands and tin octoate were tested (see Table 10).

The polymerisation activities of zinc complexes with guanidine–pyridine hybrid ligands **C1–C10** depend on the nature of the anionic component of the zinc salt in the complex and on whether the coordinated ligand contains a pyridine or a quinoline unit.

The zinc chloride complexes **C3** and **C4**, both containing a quinoline unit, show no ability to catalyse the polymerisation of D,L-lactide, but the corresponding complexes **C1** and **C2**, both exhibiting a pyridine unit, demonstrate good or very good polymerisation properties. In the case of acetate-containing complexes **C5–C8** the beneficial effect of a pyridine unit in the coordinated ligand on the ability to act as initiator in the ROP of lactide is also detected. Though the catalytic properties of the complexes with a coordinated pyridine ligand that additionally contain chlorido ligands are more favourable than those that contain acetate instead of chloride, in the case of complexes with a coordinated quinoline ligand it is the other way round. However the most auspicious candidates for highly active catalysts in the ROP of D,L-lactide are triflate-containing complexes **C9** and **C10**. They combine almost quantitative yields with high molecular weight up to 176000 g mol^{-1}. Their outstanding catalytic activities result presumably from their structural properties (accessibility to the zinc centre) and enhanced Lewis acidity. Seemingly, the weak coordination of the triflate anion favours attachment of lactide and therefore accelerates the reaction. The comparison of the guanidine–pyridine zinc system with the bis-guanidine zinc system to evaluate the strategy of substitution of one guanidine by a pyridine unit reveals at first sight no obvious trend. The zinc bis-guanidine complexes $[Zn(DMEG_2e)Cl_2]$, $[Zn(DMEG_2e)(CH_3COO)_2]$ and $[Zn(DMEG_2e)_2][CF_3SO_3]_2$[17] exhibit higher polymerisation activities than **C3–C8**, but **C1** and **C2** show higher and **C9** and **C10** much higher activities.

To classify the polymerisation activity of the guanidine–pyridine zinc system, the standard catalyst for industrial PLA production, tin octoate, was examined under the same reaction conditions. The tin compound leads to almost quantitative yields but the molecular weights of the obtained polymers (47000–80000 g mol^{-1}, see Table 10) are lower than those for **C2** and significantly smaller than those for **C9** and **C10**.

In addition, not only the structure of the used catalyst is important for the polymerisation process but also the reac-

Table 9. Polymerisation of D,L-lactide initiated by **C1–C10**.

Initiator	T [°C]	t [h]	M/I	Yield [%]	M_w [g mol^{-1}]	PDI
C1	130	24	500	55	67000	1.95
C1	150	24	500	74	44000	2.15
C1	150	48	500	88	46000	2.09
C2	130	24	500	73	94000	2.19
C2	150	24	500	83	54000	2.11
C2	150	24	1000	67	62000	2.32
C2	150	48	500	91	48000	2.20
C3	130	24	500	0	–	–
C3	150	24	500	0	–	–
C3	150	48	500	0	–	–
C4	130	24	500	0	–	–
C4	150	24	500	0	–	–
C4	150	48	500	0	–	–
C5	130	24	500	58	22000	2.51
C5	150	24	500	76	21000	2.37
C5	150	48	500	73	19000	2.48
C6	130	24	500	78	27000	2.07
C6	150	24	500	73	13000	1.99
C6	150	48	500	63	11000	2.26
C7	130	24	500	7	14000	2.73
C7	150	24	500	36	12000	2.36
C7	150	48	500	58	17000	1.96
C8	130	24	500	0	–	–
C8	150	24	500	2	12000	2.00
C8	150	48	500	41	19000	2.14
C9	130	24	500	67	176000	1.99
C9	150	24	500	92	162000	2.05
C9	150	24	1000	80	154000	2.25
C9	150	48	500	93	157000	1.96
C10	130	24	500	95	106000	1.91
C10	150	24	500	93	155000	2.16
C10	150	24	1000	94	153000	2.30
C10	150	48	500	93	102000	2.06

tion conditions are relevant. In most cases the lower temperature of 130 °C leads to higher molecular masses but slightly lower yields. Increasing the reaction time from 24 to 48 h often does not improve the conversion, nor does it increase the molecular weight of the obtained polymers. On the contrary, a decrease in yield and molecular weight can be observed in several cases. We already reported this effect for polymerisation experiments conducted with bis-guanidine complexes,[17] which may be caused by side reactions such as interchain or intrachain transesterification resulting in a chain-transfer reaction.[36]

To exclude the possibility that the complexes decompose in the polymer melt and the single components are the real initiators in the ring-opening polymerisation of lactide, the catalytic properties of the guanidine–pyridine hybrid ligands **L1**–**L4** and zinc salts $ZnCl_2$, $Zn(CH_3COO)_2$ and $Zn(CF_3SO_3)_2$ were tested (Table 10). The catalytic activities of

Table 10. Polymerisation of D,L-lactide initiated by **L1**–**L4**, $ZnCl_2$, $Zn(CH_3COO)_2$, $Zn(CF_3SO_3)_2$ and $SnOct_2$.

Initiator	T [°C]	t [h]	M/I	Yield [%]	M_w [g mol^{-1}]	PDI
None	165	24	–	0	–	–
L1	130	24	500	0	–	–
L1	150	24	500	0	–	–
L1	150	48	500	<1	–	–
L2	130	24	500	0	–	–
L2	150	24	500	0	–	–
L2	150	48	500	26	9000	2.00
L3	130	24	500	0	–	–
L3	150	24	500	0	–	–
L3	150	48	500	47	9000	1.93
L4	130	24	500	0	–	–
L4	150	24	500	0	–	–
L4	150	48	500	32	9000	2.40
$ZnCl_2$	130	24	500	0	–	–
$ZnCl_2$	150	24	500	42	34000	2.36
$ZnCl_2$	150	48	500	85	45000	2.42
$Zn(CH_3COO)_2$	130	24	500	42	134000	2.11
$Zn(CH_3COO)_2$	150	24	500	69	130000	2.09
$Zn(CH_3COO)_2$	150	48	500	84	117000	2.17
$Zn(CF_3SO_3)_2$	130	24	500	0	–	–
$Zn(CF_3SO_3)_2$	150	24	500	0	–	–
$Zn(CF_3SO_3)_2$	150	48	500	0	–	–
$SnOct_2$	130	24	500	100	80000	1.91
$SnOct_2$	150	24	500	98	47000	1.86
$SnOct_2$	150	48	500	93	37000	2.01

the guanidine–pyridine hybrid ligands are markedly lower than those of the examined complexes. In a different context, guanidines have already been reported as effective organocatalysts for the ring-opening polymerisation of cyclic esters.[37] Ligand **L1** is almost inactive and **L2**–**L4** reach an average yield of only 35% with molecular weights of 9000 g mol^{-1} at 150°C and 48 h polymerisation time; under the other conditions they show no polymerisation activity at all.

It is noteworthy that zinc chloride is inactive at 130 °C but at 150 °C gives results that are comparable to or worse than those of **C1**. Complex **C2** always shows better polymerisation activity than zinc chloride. On the other hand, the catalytic performance of zinc acetate is higher than those of all examined complexes containing zinc acetate. Interestingly, zinc triflate shows no catalytic activity at all in the ROP of lactide although the most active zinc complexes of guanidine–pyridine hybrid ligands contain this zinc salt. Nevertheless, all results show no indication that the complexes decompose in the polymer melt and that the single components may be the true initiators in the ring-opening polymerisation of lactide.

The structural characteristics of the synthesised polymers were studied by correlating their intrinsic viscosities with the molecular weight M. For large polymers this is described by the Mark–Houwink equation (1).[38]

$$[\eta] = KM^{\alpha} \quad (1)$$

Figure 8 shows Mark–Houwink plots of selected PLAs obtained by ROP with **C1**, **C2**, **C5**–**C10**, $ZnCl_2$, $Zn(CH_3COO)_2$, $Sn(Oct)_2$ and bis-guanidine complexes $[Zn(DMEG_2e)Cl_2]$,

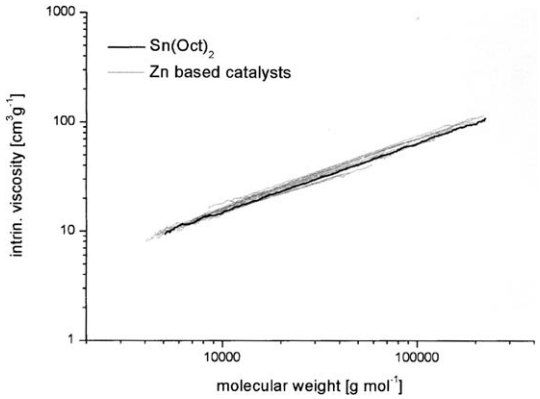

Figure 8. Mark–Houwink plot of selected PLAs obtained by ROP with zinc-based catalysts and stannous octoate. The calculated mean values of α and K in THF at 35 °C are 0.588 and 0.0674, respectively.

$[Zn(DMEG_2e)][CH_3COO]_2$ and $[Zn(DMEG_2e)_2][CF_3SO_3]_2$.[17] All plots show linear behaviour and the identical trends for all examined polymers indicate that the obtained PLA samples are structurally homogeneous and linear. Hence, the structure of the examined polymer is independent of the used initiator. The averaged values for the Mark–Houwink constants of polymers obtained by using the new ligands at 35 °C in THF were calculated to $\alpha = 0.59$ and $K = 0.067$. These values agree with those published earlier for PLAs obtained with bis-guanidine zinc complexes.[17] Comparable values for different temperatures and solvents have already been reported.[7,39]

Especially complexes **C9** and **C10** are highly active polymerisation catalysts in step with current industrial practice. They tolerate air, moisture and impurities in lactide and are soluble in organic solvents and molten lactide. The obtained polymers have high molecular masses and a relatively narrow molecular weight distribution. Intriguingly, the ROP

of lactide is catalysed without the presence of a co-initiator such as alcohols.[2,6] Furthermore, no alkoxide groups are required to attack the carbonyl group of lactide. The enhanced Lewis acidity of the zinc atoms is presumably the more important factor for the coordination and activation of lactide.

The reported class of zinc complexes offers a number of advantages: straightforward catalyst synthesis, easy and robust handling, high polymer yields and homogeneous polymers with high molecular mass.

Conclusion

We have reported on the synthesis and complete characterisation of the first examples of zinc complexes stabilised by guanidine–pyridine hybrid ligands. They proved to be active initiators in the ring-opening polymerisation of D,L-lactide with only few exceptions. Polylactides with molecular weights (M_w) up to 176000 g mol^{-1} could be obtained. This value represents a significant augmentation over bis-guanidine zinc complexes. These results corroborate our strategy of building up N-donor ligands with different donor strengths and substituents with varied steric demand. In complexes with the same ligand the activity of the initiator depends on the anionic component of the zinc salt. We found that the zinc triflate complexes are excellent catalysts for ROP of lactide. A possible explanation is that flexible coordination of one triflate anion to the zinc centre facilitates pre-coordination of the lactide molecule, while the higher positive charge at the zinc centre in comparison to the tetrahedral complexes offers higher Lewis acidity for activation of lactide. In addition, we could confirm the effect observed for bis-guanidine zinc complexes that lower temperatures allow side reactions to be avoided during polymerisation and thus give higher molecular masses. Moreover, the Mark–Houwink correlation demonstrates that the polymers obtained with the guanidine zinc complexes and the industrial standard $SnOct_2$ are linear and structurally indistinguishable. With regard to sustainability, the zinc complexes of guanidine–pyridine hybrid ligands have an advantageous combination of properties: they are non-toxic, can be stored in air without loss of activity and give PLAs with high M_w values under industrially attractive conditions. This bundle of properties makes the guanidine/zinc systems an excellent and application-oriented class of catalysts for the ring-opening polymerisation of lactide. Further investigations will focus on the kinetics of the polymerisation process and a mechanism of D,L-lactide activation and polymerisation.

Experimental Section

Materials and methods: All manipulations were performed under nitrogen (99.996%) dried with P_4O_{10} granulate by using Schlenk techniques. Solvents were purified according to literature procedures and kept under nitrogen. Zinc chloride (99.99%, Acros), zinc acetate (99.99%, Acros), zinc trifluoromethanesulfonate (98%, Aldrich), stannous octoate (95%, Aldrich) and D,L-lactide (3,6-dimethyl-1,4-dioxane-2,5-dione, Aldrich) were used as purchased. Guanidine–pyridine hybrid ligands **L1**–**L4** were prepared according to literature procedures.[26]

Physical measurements: Spectra were recorded on the following spectrometers: NMR: Bruker Avance 500. The NMR signals were calibrated to the residual signals of the deuterated solvents ($\delta_H(CDCl_3)=7.26$ ppm, $\delta_H(CD_3CN)=1.94$ ppm, $\delta_H(CD_2Cl_2)=5.32$ ppm). The DPFGSE-NOE spectra[40] were recorded with a mixing time of 0.5 s and Gaussian-shaped pulses for selective excitation. The temperature ranged from 0 to −90 °C. IR: Nicolet P510. MS (EI, 70 eV): Finnigan MAT 95; MS (CI, 100 °C, isobutane): Finnigan MAT 8200. Elemental analyses: Perkin-Elmer analysator type 2400. Microanalyses of **C9** and **C10** were performed at the Mikroanalytisches Labor, Ilse Beetz, Kronach, Germany.

Crystal structure analyses: Crystal data for **C1**–**C10** are presented in Tables 11 and 12. Data were collected on a Bruker-AXS SMART[41] APEX CCD with $Mo_{K\alpha}$ radiation ($\lambda=0.71073$ Å) and a graphite monochromator. Data reduction and absorption correction were performed

Table 11. Crystallographic data for **C1**–**C5**.

	C1	C2	C3	C4	C5
empirical formula	$C_{11}H_{16}Cl_2N_4Zn$	$C_{11}H_{18}Cl_2N_4Zn$	$C_{14}H_{16}Cl_2N_4Zn$	$C_{14}H_{18}Cl_2N_4Zn$	$C_{15}H_{22}N_4O_4Zn$
formula weight	340.55	342.56	376.58	378.59	387.74
crystal system	monoclinic	monoclinic	monoclinic	monoclinic	triclinic
space group	$P2_1/c$	$P2_1/n$	$P2_1/c$	$P2_1/c$	$P\bar{1}$
a [Å]	9.2042(5)	7.5199(10)	13.0695(5)	7.9147(3)	8.1756(4)
b [Å]	7.5147(4)	11.8762(15)	8.9289(3)	14.5789(6)	14.9245(6)
c [Å]	19.8308(12)	16.811(2)	14.6674(6)	14.1063(6)	14.9446(6)
α [°]					101.979(1)
β [°]	99.770(1)	93.763(3)	110.625(1)	100.883(1)	102.284(1)
γ [°]					97.146(1)
V [Å]^3	1351.74(13)	1498.1(3)	1601.93(10)	1598.42(11)	1715.63(13)
Z	4	4	4	4	4
ρ_{calcd} [g cm^{-3}]	1.673	1.519	1.561	1.573	1.501
μ [mm^{-1}]	2.199	1.984	1.864	1.869	1.458
T [K]	120(2)	153(2)	120(2)	120(2)	120(2)
Θ_{max} [°]	2.08 to 27.88	2.10 to 27.87	1.66 to 28.08	2.03 to 27.88	1.42 to 27.10
reflns collected	11344	12963	13895	13946	14373
independent reflns	3217	3569	3875	3818	7501
$R1$ [$I \le 2\sigma(I)$]	0.0218	0.0320	0.0226	0.0242	0.0308
$wR2$ (all data)	0.0571	0.0831	0.0599	0.0636	0.0846
largest diff. peak, hole [e Å^{-3}]	0.455, −0.241	0.494, −0.279	0.391, −0.217	0.369, −0.262	0.386, −0.256

Table 12. Crystallographic data for **C6**–**C10**.

	C6	**C7**	**C8**	**C9**	**C10**·THF
empirical formula	$C_{15}H_{24}N_4O_4Zn$	$C_{18}H_{22}N_4O_4Zn$	$C_{18}H_{24}N_4O_4Zn$	$C_{30}H_{32}F_6N_8O_6S_2Zn$	$C_{34}H_{44}F_6N_8O_7S_2Zn$
formula weight	389.75	423.77	425.78	844.13	920.26
crystal system	triclinic	monoclinic	monoclinic	monoclinic	orthorhombic
space group	$P\bar{1}$	$P2_1/c$	$P2_1/c$	$P2_1/n$	$Pca2_1$
a [Å]	8.1208(12)	16.0992(7)	15.4699(6)	15.4611(19)	18.2063(17)
b [Å]	8.1387(12)	8.4523(4)	7.9664(3)	13.7377(17)	14.7468(13)
c [Å]	8.3914(13)	14.1361(6)	17.1668(7)	16.910(2)	29.956(3)
α [°]	72.865(3)				
β [°]	65.409(3)	109.804(1)	115.422(1)	98.624(3)	
γ [°]	62.144(3)				
V [Å^3]	442.40(12)	1809.81(14)	1910.77(13)	3551.1(8)	8042.7(13)
Z	1	4	4	4	8
ρ_{calcd} [g cm^{-3}]	1.463	1.555	1.480	1.579	1.520
μ [mm^{-1}]	1.414	1.390	1.317	0.895	0.799
temperature [K]	120(2)	120(2)	120(2)	120(2)	120(2)
Θ_{max} [°]	2.69 to 26.37	1.34 to 27.88	1.46 to 27.88	1.66 to 27.88	1.36 to 27.88
reflns collected	3403	15384	16261	30999	69596
independent reflns	2794	4304	4531	8471	18098
$R1$ [$I \leq 2\sigma(I)$]	0.0263	0.0282	0.0267	0.0622	0.0471
$wR2$ (all data)	0.0633	0.0791	0.0749	0.1712	0.1126
largest diff. peak, hole [e Å^{-3}]	0.319, −0.293	0.468, −0.340	0.390, −0.225	1.197, −1.079	0.535, −0.390

with SAINT and SADABS.[41] The structures were solved by direct and conventional Fourier methods, and all non-hydrogen atoms refined anisotropically by full-matrix least-squares techniques based on F^2 (SHELXTL[41]). Hydrogen atoms were derived from difference Fourier maps and placed at idealised positions, riding on their parent C atoms, with isotropic displacement parameters $U_{iso}(H) = 1.2\,U_{eq}(C)$ and $1.5\,U_{eq}$-(C_{methyl}). All methyl groups were allowed to rotate but not to tip. Structures of **C5** and **C10** exhibit two independent molecules per asymmetric unit each. CCDC-699072 (**C1**), CCDC-699077 (**C2**), CCDC-699070 (**C3**), CCDC-699071 (**C4**), CCDC-699075 (**C5**), CCDC-699076 (**C6**), CCDC-699074 (**C7**), CCDC-699073 (**C8**), CCDC-699078 (**C9**) and CCDC-699079 (**C10**·THF) contain the supplementary crystallographic data for this paper. These data can be obtained free of charge from The Cambridge Crystallographic Data Centre via www.ccdc.cam.ac.uk/data_request/cif

Computational details: Density functional theory (DFT) calculations were performed with the program suite Gaussian 03.[31] The geometries of the complexes and ligands were optimised (Tables S1–S6 in the Supporting Information) by using the B3LYP[42] hybrid DFT functional and the 6-31g(d) and 6-31g+(d) basis sets implemented in Gaussian on all atoms. Tight conversion criteria were applied. The starting geometries of complexes **C1**–**C10** were generated from their crystal structures, whereas the starting geometries of ligands **L1**–**L4** were derived from their optimised complexes.

Frequency calculations confirmed the stationary points to be minima. Electronic energies for gas-phase optimised structures **C5a** and **C5b** were computed by using the BLYP functional and a 6-311g(d) basis set on the Zn, O and N atoms and a 6-31g(d) basis set on the remaining atoms. The Mulliken charge of each atom was calculated by a Mulliken population analysis.

Gel permeation chromatography: To obtain Mark–Houwink constants of the PLA samples obtained by ROP with $SnOct_2$ and the zinc complexes of guanidine–pyridine hybrid ligands, GPC measurements were performed on a Waters GPC 2000 instrument equipped with a precolumn (10 μm) and a combination of three PSS-SDV columns (10^6, 10^5, 10^3 Å). The detection system included an integrated refractive index (RI) detector and an integrated viscosity detector H502B (Viscotek). All measurements were performed at 35 °C with THF as eluent. The flow rate was 1 mL min^{-1}. Sample concentrations were 2–3 g L^{-1}. Molecular weight analysis was based on a universal calibration, carried out with polystyrene standards (Polymer Standard Service) in THF at 35 °C. Use of the universal calibration gave absolute values for the molecular weight, which are discussed as weight-average molar mass values M_w and as the polydispersity index ($PDI = M_w/M_n$ where M_n is the number-average molar mass) which measures the width of the molecular weight distribution. The data are summarised in Table S7 (see the Supporting Information).

The whole series of polymers was investigated with a different GPC set-up: A combination of PSS SDV columns with porosities of 10^5 and 10^3 Å was used together with a HPLC pump (L6200, Merck Hitachi) and a refractive index detector (Smartline RI Detector 2300, Knauer). THF was used as mobile phase at a flow rate of 1 mL min^{-1}. The instrument was calibrated with standard polystyrene samples, for which the following Mark–Houwink constants could be taken from the literature ($K_{PS} = 0.011$ mL g^{-1}, $\alpha_{PS} = 0.725$).[43] Hence, the obtained values for the molecular weight and molecular weight distribution are polystyrene-analogous. To obtain absolute values, $K_{PLA} = 0.053$ mL g^{-1}, $\alpha_{PLA} = 0.610$ were chosen from Table S7 (see Supporting Information) as representative Mark–Houwink constants for PLA. Combination of these two sets of data enables equalisation[38] of the hydrodynamically effective volumes of PS and PLA, $V_{h,PS}$ and $V_{h,PLA}$, at any elution volume according to Equation (2)

$$V_{h,PS} = K_{PS}M^{\alpha(PS)}M = K_{PS}M^{\alpha(PS)+1} = V_{h,PLA} = K_{PLA}M^{\alpha(PLA)+1} \quad (2)$$

General synthesis of zinc complexes with guanidine–pyridine hybrid ligands: A solution of the ligand (1.1 mmol) in MeCN or THF was added to a suspension of 1 mmol of ($ZnCl_2$, $Zn(CH_3COO)_2$ or $Zn(CF_3SO_3)$ in a dry aprotic solvent (MeCN, THF), with stirring. The resulting reaction mixture was stirred for 20 min. In the case of a clear solution (**C5**–**C8**, **C10**), single crystals could be obtained by diffusion of diethyl ether or diisopropyl ether. When the complex precipitated (**C1**–**C4**, **C9**), the reaction mixture was slowly heated under reflux to give a clear solution. Crystals could be obtained by slowly cooling to room temperature.

[Zn(DMEGpy)Cl$_2$] (C1) Colourless crystals (0.32 g, 94%); m.p. 258 °C; ^{1}H NMR (500 MHz, CD_3CN, 25 °C): $\delta = 3.09$ (s, 6H; CH_3), 3.50 (s, 4H; CH_2), 4.89 (s, 2H; CH_2), 7.56 (m, 2H; 2CH), 8.04 (m, 1H; CH), 8.55 ppm (m, 1H; CH); ^{13}C NMR (125 MHz, CD_3CN, 25 °C): $\delta = 37.5$ (CH_3), 50.5 (CH_2), 52.2 (CH_2), 123.7 (CH), 125.0 (CH), 141.3 (CH), 147.7 (CH), 158.9 (C), 164.7 (C_{gua}); IR (KBr): $\tilde{\nu} = 2935$ m (ν(C–H_{aliph})), 2870 m (ν(C–H_{aliph})), 1610 m, 1587 vs (ν(C=N)), 1570 s, 1514 m, 1489 m, 1458 m, 1441 m, 1412 m, 1388 m, 1369 m, 1300 m, 1284 m, 1215 w, 1157 vw, 1107 vw, 1088 vw, 1045 m, 1026 w, 970 vw, 793 m, 762 m, 725 m, 714 w, 646 w, 577 vw, 474 vw, 415 cm^{-1} w; EIMS: m/z (%, assignment): 339 (2, [M^+]),

304 (10, [$M^+-{}^{35}Cl$]), 302 (8, [$M^+-{}^{37}Cl$]), 204 (89, [M^+-ZnCl_2]), 126 (100, [$M^+-C_5H_4N-ZnCl_2$]), 112 (32, [$M^+-C_6H_6N-ZnCl_2$]), 92 (18, [$C_6H_6N^+$]), 56 (14); elemental analysis calcd (%) for $C_{11}H_{16}N_4ZnCl_2$: C 38.76, H 4.70, N 16.44; found: C 39.76, H 4.70, N 16.44.

[Zn(TMGpy)Cl$_2$] (C2): Colourless crystals (0.22 g, 64%); m.p. 190°C; ^{1}H NMR (500 MHz, CD_3CN, 25°C): $\delta=2.77$ (s, 6H; CH_3), 2.98 (s, 6H; CH_3), 4.59 (s, 2H; CH_2), 7.54 (m, 2H; 2 CH), 8.03 (m, 1H; CH), 8.50 ppm (m, 1H; CH); ^{13}C NMR (125 MHz, CD_3CN, 25°C): $\delta=39.1$ (CH_3), 51.8 (CH_2), 122.8 (CH), 123.9 (CH), 140.1 (CH), 147.0 (CH), 158.6 (C), 166.1 (C_{gua}); IR (KBr): $\tilde{\nu}=3302$ vw (ν(C−H_{arom})), 3122 vw (ν(C−H_{arom})), 2993 vw (ν(C−H_{aliph})), 2945 w (ν(C−H_{aliph})), 2891 w (ν(C−H_{aliph})), 2844 vw (ν(C−H_{aliph})), 2796 vw (ν(C−H_{aliph})), 1608 m (ν(C=N)), 1574 s (ν(C=N)), 1558 vs (ν(C=N)), 1537 s (ν(C=N)), 1483 m, 1473 m, 1441 m, 1425 m, 1410 m, 1396 m, 1356 m, 1286 m, 1238 m, 1221 w, 1163 m, 1140 m, 1105 w, 1078 w, 1063 w, 1053 w, 1026 m, 978 vw, 906 m, 839 w, 773 m, 760 m, 715 w, 650 w, 623 w, 594 w, 553 cm^{-1} vw; EIMS: *m/z* (%, assignment): 342 (4, [M^+]), 307 (2, [$M^+-{}^{35}Cl$]), 305 (4, [$M^+-{}^{37}Cl$]), 249 (73), 224 (80), 206 (35, [M^+-ZnCl_2]), 162 (23, [$M^+-ZnCl_2-N(CH_3)_2$]), 147 (15, [$M^+-ZnCl_2-N(CH_3)_2-CH_3$]), 126 (73, [$CH_2NC\{N(CH_3)_2\}_2^+-2H$]), 121 (36), 119 (100, [$M^+-ZnCl_2-2N(CH_3)_2+H$]), 108 (95, [$M^+-ZnCl_2-C\{N(CH_3)_2\}_2+2H$]), 107 (89, [$M^+-ZnCl_2-C\{N(CH_3)_2\}_2+H$]), 92 (53, [$M^+-ZnCl_2-NC\{N(CH_3)_2\}_2$]), 87 (51), 85 (39, [$CH_2NC(N(CH_3)_2)^+$+H]), 80 (96, [$C_5NH_4^+$+2H]), 79 (90, [$C_5NH_4^+$+H]), 71 (38, [NCN-$(CH_3)_2^+$+H]), 58 (78, [$C(N(CH_3)_2)^+$+2H]), 52 (71); elemental analysis calcd (%) for $C_{11}H_{18}N_4ZnCl_2$: C 38.53, H 5.25, N 16.35; found: C 38.77, H 5.20, N 15.90.

[Zn(DMEGqu)Cl$_2$] (C3): Yellow crystals (0.36 g, 96%); m.p. 281°C; ^{1}H NMR (500 MHz, CD_3CN, 25°C): $\delta=2.90$ (s, 6H; CH_3), 3.70 (m, 4H; CH_2), 7.17 (dd, 1H; CH, $^3J=7.7$, $^4J=1.1$ Hz), 7.52 (dd, 1H; CH, $^3J=8.1$, $^4J=1.1$ Hz), 7.62 (dd, 1H; CH, $^3J=8.1$, $^3J=7.7$ Hz), 7.74 (dd, 1H; CH, $^3J=8.4$, $^3J=4.6$ Hz), 8.57 (dd, 1H; CH, $^3J=8.4$, $^4J=1.5$ Hz), 8.81 ppm (dd, 1H; CH, $^3J=4.6$, $^4J=1.5$ Hz); ^{13}C NMR (125 MHz, CD_3CN, 25°C): $\delta=34.9$ (CH_3), 48.2 (CH_2), 117.7 (CH), 118.5 (CH), 122.5 (CH), 128.7 (CH), 129.6 (C), 138.3 (C), 140.3 (CH), 142.8 (C), 147.7 (CH), 164.7 ppm (C_{gua}); IR (KBr): $\tilde{\nu}=3039$ w (ν(C−H_{arom})), 2976 w (ν(C−H_{aliph})), 2945 w (ν(C−H_{aliph})), 2926 w (ν(C−H_{aliph})), 2877 w (ν(C−H_{aliph})), 1556 vs (ν(C=N)), 1500 s, 1469 m, 1415 m, 1410 m, 1394 m, 1383 m, 1325 m, 1284 m, 1236 w, 1200 vw, 1167 vw, 1138 vw, 1103 w, 1078 vw, 1045 vw, 1026 m, 978 w, 912 vw, 829 w, 816 w, 781 m, 760 w, 698 vw, 663 vw, 636 w, 611 vw, 579 w, 536 vw, 472 cm^{-1} vw; EIMS: *m/z* (%, assignment): 380 (2, [M^+]: $C_{14}H_{16}N_4{}^{37}Cl_2{}^{66}Zn$, $C_{14}H_{16}N_4{}^{35}Cl^{37}Cl^{68}Zn$), 379 (1, [$M^+$]: $C_{13}{}^{13}CH_{16}N_4{}^{35}Cl^{37}Cl^{66}Zn$, $C_{14}H_{16}N_4{}^{35}Cl^{37}Cl^{67}Zn$, $C_{13}{}^{13}CH_{16}N_4{}^{35}Cl_2{}^{68}Zn$), 378 (5, [$M^+$]: $C_{14}H_{16}N_4{}^{35}Cl_2{}^{68}Zn$), 377 (1, [$M^+$]: $C_{14}H_{16}N_4{}^{37}Cl_2{}^{64}Zn$, $C_{14}H_{16}N_4{}^{35}Cl^{37}Cl^{66}Zn$), 376 (6, [$M^+$]: $C_{14}H_{16}N_4{}^{35}Cl_2{}^{66}Zn$, $C_{14}H_{16}N_4{}^{35}Cl^{37}Cl^{64}Zn$), 375 (1, [$M^+$]: $C_{13}{}^{13}CH_{16}N_4{}^{35}Cl_2{}^{64}Zn$), 374 (5, [$M$]$^+$: $C_{14}H_{16}N_4{}^{35}Cl_2{}^{64}Zn$), 341 (28, [$M^+-{}^{35}Cl$]), 339 (34, [$M^+-{}^{37}Cl$]), 240 (100, [$M^+-ZnCl_2$]), 197 (11, [$M^+-(CH_3)NCH_2-ZnCl_2$]), 183 (36, [$M^+-C_3H_7N-ZnCl_2$]), 155 (70, [$M^+-CH_3NCH_2CH_2NCH_3-ZnCl_2$+H]), 144 (39, [$M^+-C_5H_{10}N_2-ZnCl_2$]), 129 (50, [$C_9H_6N^+$+H]), 98 (90, [$C_5H_{10}N_2^+$]), 69 (23); elemental analysis calcd (%) for $C_{14}H_{16}N_4ZnCl_2$: C 44.60, H 4.25, N 14.87; found: C 44.72, H 4.17, N 14.87.

[Zn(TMGqu)Cl$_2$](C4) Yellow crystals (0.33 g, 87%); m.p. 292°C; ^{1}H NMR (500 MHz, CD_3CN, 25°C): $\delta=2.82$ (s, 6H; CH_3), 3.05 (s, 6H; CH_3), 7.03 (dd, 1H; CH, $^3J=7.5$, $^4J=1.2$ Hz), 7.61 (dd, 1H; CH, $^3J=8.2$, $^4J=1.2$ Hz), 7.67 (dd, 1H; CH, $^3J=8.2$, $^3J=7.5$ Hz), 7.75 (dd, 1H; CH, $^3J=8.4$, $^3J=4.6$ Hz), 8.58 (dd, 1H; CH, $^3J=8.4$, $^4J=1.5$ Hz), 8.82 ppm (dd, 1H; CH, $^3J=4.6$, $^4J=1.5$ Hz); ^{13}C NMR (125 MHz, CD_3CN, 25°C): $\delta=39.9$ (CH_3), 117.9 (CH), 119.6 (CH), 122.6 (CH), 128.9 (CH), 129.5 (C), 138.8 (C), 140.2 (CH), 143.2 (C), 148.1 (CH), 165.5 ppm (C_{gua}); IR (KBr): $\tilde{\nu}=3041$ w (ν(C−H_{arom})), 3018 w (ν(C−H_{arom})), 3008 w (ν(C−H_{arom})), 2951 w (ν(C−H_{aliph})), 2933 w (ν(C−H_{aliph})), 2895 w (ν(C−H_{aliph})), 1560 s (ν(C=N)), 1525 vs (ν(C=N)), 1500 s, 1466 s, 1442 m, 1417 s, 1387 s, 1336 m, 1273 w, 1236 m, 1163 m, 1140 w, 1103 w, 1065 w, 1018 m, 926 vw, 831 m, 818 m, 806 w, 785 m, 756 m, 704 w, 656 vw, 631 w, 582 vw, 542 vw, 478 vw, 438 cm^{-1} vw; EIMS: *m/z* (%, assignment): 382 (3, [M^+]: $C_{14}H_{18}N_4{}^{37}Cl_2{}^{66}Zn$, $C_{14}H_{18}N_4{}^{35}Cl^{37}Cl^{68}Zn$), 381 (2, [$M^+$]: $C_{13}{}^{13}CH_{18}N_4{}^{35}Cl^{37}Cl^{66}Zn$, $C_{14}H_{18}N_4{}^{35}Cl^{37}Cl^{67}Zn$, $C_{13}{}^{13}CH_{18}N_4{}^{35}Cl_2{}^{68}Zn$), 380 (6, [$M^+$]: $C_{14}H_{18}N_4{}^{35}Cl^{37}Cl^{66}Zn$, $C_{14}H_{18}N_4{}^{37}Cl_2{}^{64}Zn$, $C_{14}H_{18}N_4{}^{35}Cl_2{}^{68}Zn$), 379 (2, [$M^+$]: $C_{14}H_{18}N_4{}^{35}Cl_2{}^{67}Zn$, $C_{13}{}^{13}CH_{18}N_4{}^{35}Cl_2{}^{66}Zn$, $C_{13}{}^{13}CH_{18}N_4{}^{35}Cl^{37}Cl^{64}Zn$), 378 (8, [$M^+$]: $C_{14}H_{18}N_4{}^{35}Cl_2{}^{66}Zn$, $C_{14}H_{18}N_4{}^{35}Cl^{37}Cl^{64}Zn$), 377 (1, [$M^+$]: $C_{13}{}^{13}CH_{18}N_4{}^{35}Cl_2{}^{64}Zn$), 376 (6, [$M^+$]: $C_{14}H_{18}N_4{}^{35}Cl_2{}^{64}Zn$), 343 (39, {$M^+-{}^{35}Cl$]), 341 (47, [$M^+-{}^{37}Cl$]), 282 (17), 242 (38, [$M^+-ZnCl_2$]), 198 (92, [$M^+-N(CH_3)_2-ZnCl_2$]), 171 (91), 155 (95), 144 (66, [$M^+-C\{N(CH_3)_2\}_2-ZnCl_2$]), 128 (54, [$M^+-C(N)(N-(CH_3)_2)_2-ZnCl_2$]), 114 (9, [$C(N)(N(CH_3)_2)_2^+$]), 100 (100, [$C\{N(CH_3)_2\}_2^+$]), 85 (37); elemental analysis calcd (%) for $C_{14}H_{18}N_4ZnCl_2$: C 44.36, H 4.75, N 14.79; found: C 44.68, H 4.82, N 14.77.

[Zn(DMEGpy)(CH$_3$COO)$_2$] (C5): Colourless crystals (0.37 g, 96%); m.p. 133°C; ^{1}H NMR (500 MHz, CD_3CN, 25°C): $\delta=1.86$ (s, 6H; CH_3), 2.98 (s, 6H; CH_3), 3.45 (s, 4H; CH_2), 4.82 (s, 2H; CH_2), 7.48 (m, 2H; 2 CH), 7.97 (m, 1H; CH), 8.76 ppm (m, 1H; CH); ^{13}C NMR (125 MHz, CD_3CN, 25°C): $\delta=21.8$ (CH_3), 35.8 (CH_3), 49.4 (CH_2), 51.2 (CH_2), 122.1 (CH), 123.2 (CH), 139.6 (CH), 148.0 (CH), 158.5 (C), 165.0 (C_{gua}), 177.2 ppm (C_{ac}); IR (KBr): $\tilde{\nu}=3072$ vw (ν(C−H_{arom})), 3033 vw (ν(C−H_{arom})), 2960 w (ν(C−H_{aliph})), 2910 m (ν(C−H_{aliph})), 2873 m (ν(C−H_{aliph})), 1616 vs, 1591 vs (ν(C=N)), 1518 m, 1493 m, 1437 m, 1412 m, 1379 s, 1327 m, 1302 m, 1290 m, 1215 w, 1163 vw, 1082 vw, 1057 w, 1041 w, 1007 w, 970 vw, 924 vw, 895 vw, 795 w, 768 m, 725 w, 675 m, 619 vw, 580 cm^{-1} vw; EIMS: *m/z* (%, assignment): 386 (19, [M^+]), 345 (3), 288 (6, [$M^+-C_5H_{10}N_2$]), 257 (9, [$M^+-CH_3NCH_2CH_2-CH_3COO$+H]), 204 (79, [$M^+-Zn(CH_3COO)_2$]), 132 (13), 126 (100, [$M^+-Zn(CH_3COO)_2-C_5H_4N$]), 112 (31, [$C_5H_{10}N_2^+$]), 98 (7, [$C_5H_{10}N_2^+$]), 92 (28, [$C_6H_6N^+$]), 78 (11, [$C_5H_4N^+$]), 69 (21, [$C_3H_5N_2^+$]), 56 (28, [$CH_3NCH_2CH_2^+-H$]); elemental analysis calcd (%) for $C_{15}H_{22}N_4O_4Zn$: C 46.42, H 5.67, N 14.44; found: C 46.14, H 5.43, N 14.17.

[Zn(TMGpy)(CH$_3$COO)$_2$] (C6) Colourless crystals (0.30 g, 76%); m.p. 160°C; ^{1}H NMR (500 MHz, $CDCl_3$, 25°C): $\delta=1.99$ (s, 6H; CH_3), 2.79 (s, 6H; CH_3), 2.94 (s, 6H; CH_3), 4.56 (s, 2H; CH_2), 7.29 (m, 1H; CH), 7.34 (t, 1H; CH, $^3J=5.6$, $^3J=6.3$ Hz), 7.79 (t, 1H; CH, $^3J=7.0$, $^3J=7.5$ Hz), 8.78 ppm (m, 1H; CH); ^{13}C NMR (125 MHz, $CDCl_3$, 25°C): $\delta=22.7$ (CH_3), 39.3 (CH_3), 39.8 (CH_3), 52.5 (CH_2), 122.6 (CH), 123.2 (CH), 138.9 (CH), 148.6 (CH), 158.1 (C), 165.8 (C_{gua}), 178.9 ppm (C_{ac}); IR (KBr): $\tilde{\nu}=3068$ w (ν(C−H_{arom})), 3024 w (ν(C−H_{arom})), 2995 w (ν(C−H_{aliph})), 2941 w (ν(C−H_{aliph})), 2902 w (ν(C−H_{aliph})), 2893 w (ν(C−H_{aliph})), 2862 w (ν(C−H_{aliph})), 2833 w (ν(C−H_{aliph})), 1618 s, 1608 s, 1593 m, 1574 s, 1560 vs (ν(C=N)), 1541 m, 1489 m, 1473 m, 1441 m, 1427 m, 1396 s, 1354 m, 1327 m, 1296 m, 1254 w, 1236 w, 1165 w, 1147 w, 1109 vw, 1078 w, 1057 w, 1026 w, 987 vw, 918 vw, 908 w, 833 vw, 779 w, 769 vw, 742 vw, 717 vw, 675 m, 650 w, 617 w, 594 cm^{-1} w; EIMS: *m/z* (%, assignment): 388 (36, [M^+]), 329 (9, [M^+-CH_3COO]), 206 (81, [$M^+-Zn(CH_3COO)_2$]), 162 (88, [$M^+-Zn-(CH_3COO)_2-N(CH_3)_2$)], 147 (69, [$M^+-Zn(CH_3COO)_2-N(CH_3)_2-CH_3$]), 93 (90, [$M^+-Zn(CH_3COO)_2-NC\{N(CH_3)_2\}_2$+H]), 92 (100, [$M^+-Zn-(CH_3COO)_2-NC\{N(CH_3)_2\}_2$]), 85 (86, [$CH_2NC(N(CH_3)_2)^+$+2H]), 65 (77); elemental analysis calcd (%) for $C_{15}H_{24}N_4O_4Zn$: C 46.18, H 6.16, N 14.37; found: C 46.23, H 6.25, N 14.30.

[Zn(DMEGqu)(CH$_3$COO)$_2$] (C7): Yellow crystals (0.42 g, 99%); m.p. 197°; ^{1}H NMR (500 MHz, CD_3CN, 25°C): $\delta=1.86$ (s, 6H; CH_3), 2.82 (s, 6H; CH_3), 3.61 (m, 2H; CH_2), 3.75 (m, 2H; CH_2), 7.03 (dd, 1H; CH, $^3J=7.7$, $^4J=1.1$ Hz), 7.42 (dd, 1H; CH, $^3J=8.2$, $^4J=1.1$ Hz), 7.55 (dd, 1H; CH, $^3J=8.2$, $^3J=7.7$ Hz), 7.68 (dd, 1H; CH, $^3J=8.3$, $^3J=4.6$ Hz), 8.48 (dd, 1H; CH, $^3J=8.3$, $^4J=1.6$ Hz), 8.96 ppm (dd, 1H; CH, $^3J=4.6$, $^4J=1.6$ Hz); ^{13}C NMR (125 MHz, CD_3CN, 25°C): $\delta=21.4$ (CH_3), 34.1 (CH_3), 48.0 (CH_2), 116.1 (CH), 117.3 (CH), 122.1 (CH), 128.4 (CH), 129.4 (C), 138.3 (C), 139.6 (CH), 143.7 (C), 148.3 (CH), 164.9 (C_{gua}), 178.0 ppm (C_{ac}); IR (KBr): $\tilde{\nu}=3060$ w (ν(C−H_{arom})), 3043 w (ν(C−H_{arom})), 2987 w (ν(C−H_{aliph})), 2960 w (ν(C−H_{aliph})), 2929 w (ν(C−H_{aliph})), 2891 w (ν(C−H_{aliph})), 1576 vs (ν(C=N)), 1568 vs (ν(C=N)), 1502 s, 1483 m, 1466 m, 1417 s, 1392 vs, 1327 m, 1300 m, 1240 m, 1209 w, 1173 vw, 1134 vw, 1103 w, 1043 w, 1026 m, 978 w, 930 vw, 910 vw, 820 m, 806 m, 785 m, 773 w, 756 w, 673 m, 640 w, 617 w, 580 w, 534 cm^{-1} w; EIMS: *m/z* (%, assignment): 424 (2, [M^++H]), 394 (3, [M^+-2CH_3]), 389 (24), 387 (19), 365 (5), 341 (2), 287 (2), 256 (9), 240 (100, [$M^+-Zn(CH_3COO)_2$]), 198 (18, [$M^+-(CH_3)NCH_2-Zn(CH_3COO)_2$+H]), 183 (12, [$M^+-C_3H_7N-Zn(CH_3COO)_2$]), 155 (39, [$M^+-CH_3NCH_2CH_2NCH_3-Zn-(CH_3COO)_2$+H]), 144 (13, [$M^+-C_5H_{10}N_2-Zn(CH_3COO)_2$]), 129 (21, [$C_9H_6N^+$+H]), 98 (27, [$C_5H_{10}N_2$]$^+$), 60 (8, [$CH_3COO^-$+H]); elemental

analysis calcd (%) for $C_{18}H_{22}N_4O_4Zn$: C 50.97, H 5.19, N 13.21; found: C 51.01, H 5.21, N 13.02.

[Zn(TMGqu)(CH$_3$COO)$_2$] (C8): Yellow crystals (0.42 g, 99%); m.p. 204°C; ^{1}H NMR (500 MHz, CD_3CN, 25°C): $\delta = 1.86$ (s, 6H; CH_3), 2.76 (s, 6H; CH_3), 3.01 (s, 6H; CH_3), 6.88 (dd, 1H; CH, $^3J = 7.6$, $^4J = 1.2$ Hz), 7.51 (dd, 1H; CH, $^3J = 8.2$, $^4J = 1.2$ Hz), 7.59 (dd, 1H; CH, $^3J = 8.2$, $^3J = 7.6$ Hz), 7.68 (dd, 1H; CH, $^3J = 8.4$, $^3J = 4.6$ Hz), 8.49 (dd, 1H; CH, $^3J = 8.4$, $^4J = 1.6$ Hz), 8.95 ppm (dd, 1H; CH, $^3J = 4.6$, $^4J = 1.6$ Hz); ^{13}C NMR (125 MHz, CD_3CN, 25°C): $\delta = 21.3$ (CH_3), 38.8 (CH_3), 40.2 (CH_3), 116.5 (CH), 118.6 (CH), 122.2 (CH), 128.5 (CH), 129.2 (C), 138.7 (C), 139.4 (CH), 144.1 (C), 148.6 (CH), 165.8 (C_{gua}), 178.1 ppm (C_{ac}); IR (KBr): $\tilde{\nu} =$ 3064 w (ν(C–H_{arom})), 3012 w (ν(C–H_{arom})), 2968 m (ν(C–H_{aliph})), 2929 m (ν(C–H_{aliph})), 2897 w (ν(C–H_{aliph})), 1616 vs (ν(C=N)), 1597 s (ν(C=N)), 1570 s (ν(C=N)), 1523 vs, 1500 s, 1468 m, 1556 m, 1412 s, 1387 vs, 1329 s, 1275 m, 1232 m, 1165 m, 1140 w, 1128 w, 1101 w, 1066 w, 1056 w, 1041 w, 1018 m, 951 vw, 922 w, 903 vw, 876 vw, 835 m, 816 m, 787 m, 758 w, 742 m, 702 w, 675 m, 617 w, 579 vw, 544 cm^{-1} vw; CIMS (*m*/*z*, assignment): 424 (0.5, [M^+–H]), 365 (0.5, [M^+–CH_3COO]), 300 (4), 299 (17), 257 (29), 243 (100, [M^+–Zn(CH_3COO)$_2$+H]), 242 (99, [M^+–Zn(CH_3COO)$_2$]), 201 (5), 198 (4, [M^+–Zn(CH_3COO)$_2$–N(CH_3)$_2$]), 143 (1, [M^+–Zn(CH_3COO)$_2$–C{N(CH_3)$_2$}$_2$+H]), 57 (90); elemental analysis calcd (%) for $C_{18}H_{24}N_4O_4Zn$: C 50.73, H 5.64, N 13.15; found: C 50.89, H 5.60, N 12.83.

[Zn(DMEGqu)$_2$(CF$_3$SO$_3$)][CF$_3$SO$_3$] (C9): Yellow crystals (0.31 g, 73%); m.p. 234°C; ^{1}H NMR (500 MHz, CD_3CN, 25°C): $\delta = 2.56$ (s, 12H; CH_3), 3.48 (s, 4H; CH_2), 3.72 (s, 4H; CH_2), 7.16 (dd, 2H; CH, $^3J = 7.7$, $^4J =$ 1.1 Hz), 7.60 (dd, 2H; CH, $^3J = 8.2$, $^4J = 1.1$ Hz), 7.68 (dd, 2H; CH, $^3J =$ 8.2, $^3J = 7.7$ Hz), 7.85 (dd, 2H; CH, $^3J = 8.3$, $^3J = 4.7$ Hz), 8.69 (dd, 2H; CH, $^3J = 8.3$, $^4J = 1.5$ Hz), 8.78 ppm (dd, 2H; CH, $^3J = 4.7$, $^4J = 1.5$ Hz); ^{13}C NMR (125 MHz, CD_3CN, 25°C): $\delta = 33.9$ (CH_3), 47.5 (CH_2), 116.2 (CH), 118.2 (CH), 122.2 (C_{tf}), 122.4 (CH), 128.9 (CH), 129.7 (C), 137.7 (C), 141.0 (CH), 142.1 (C), 148.1 (CH), 164.4 ppm (C_{gua}); IR (KBr): $\tilde{\nu} =$ 3057 vw (ν(C–H_{arom})), 2960 vw (ν(C–H_{aliph})), 2935 vw (ν(C–H_{aliph})), 2889 w (ν(C–H_{aliph})), 1597 m (ν(C=N)), 1558 s (ν(C=N)), 1504 m, 1468 m, 1419 m, 1396 m, 1327 m, 1302 m, 1267 vs, 1232 m, 1225 m, 1174 m, 1155 m, 1103 w, 1032 s, 1024 s, 976 w, 912 vw, 827 m, 806 w, 789 m, 771 w, 756 w, 692 w, 636 m, 582 w, 573 w, 536 vw, 517 cm^{-1} w; EIMS: *m*/*z* (%, assignment): 693 (1, [M^+–CF_3SO_3]), 602 (6), 453 (27, [M^+ –CF_3SO_3–$C_{14}H_{16}N_4$]), 240 (100, [$C_{14}H_{16}N_4$]$^+$), 183 (20, [$C_{14}H_{16}N_4^+$ –$CH_3NCH_2CH_2$]), 169 (18), 155 (63, [$C_{10}H_6N_2^+$+H]), 142 (19, [$C_{14}H_{16}N_4^+$ –$C_5H_{10}N_2$]), 129 (33, [$C_9H_6N_2^+$+H]), 98 (75, [$C_5H_{10}N_2$]$^+$); elemental analysis calcd (%) for $C_{30}H_{32}N_8O_6F_6S_2Zn$: C 42.58, H 3.78, N 13.25; found: C 42.66, H 3.89, N 13.17.

[Zn(TMGqu)$_2$(CF$_3$SO$_3$)][CF$_3$SO$_3$] (C10) Yellow crystals (0.46 g, 99%); m.p. 225°C; ^{1}H NMR (500 MHz, CD_3CN, 25°C): $\delta = 2.47$ (s, 12H; CH_3), 2.76 (s, 6H; CH_3), 3.07 (s, 6H; CH_3), 7.02 (dd, 2H; CH, $^3J = 7.5$, $^4J =$ 1.3 Hz), 7.71 (dd, 2H; CH, $^3J = 8.2$, $^4J = 1.3$ Hz), 7.75 (dd, 2H; CH, $^3J =$ 8.2, $^3J = 7.5$ Hz), 7.87 (dd, 2H; CH, $^3J = 8.4$, $^3J = 4.7$ Hz), 8.72 (dd, 2H; CH, $^3J = 8.4$, $^4J = 1.5$ Hz), 8.75 ppm (dd, 2H; CH, $^3J = 4.7$, $^4J = 1.5$ Hz); ^{13}C NMR (125 MHz, CD_3CN, 25°C): $\delta = 39.3$ (CH_3), 39.7 (CH_3), 40.8 CH_3), 116.8 (CH), 119.6 (CH), 122.2 (C_{tf}), 122.7 (CH), 129.2 (CH), 129.6 (C), 137.8 (C), 140.9 (CH), 142.3 (C), 148.7 (CH), 165.3 ppm (C_{gua}); IR (KBr): $\tilde{\nu} = 3086$ w (ν(C–H_{arom})), 3057 w (ν(C–H_{arom})), 3012 w (ν(C–H_{arom})), 2941 m (ν(C–H_{aliph})), 2875 m (ν(C–H_{aliph})), 2808 w (ν(C–H_{aliph})), 1574 s (ν(C=N)), 1523 vs (ν(C=N)), 1502 s, 1468 s, 1425 s, 1406 s, 1387 s, 1333 s, 1275 vs, 1261 vs, 1161 s, 1103 m, 1061 m, 1030 vs, 920 w, 901 w, 839 m, 806 m, 793 m, 760 m, 702 m, 638 s, 573 m, 542 m, 517 cm^{-1} m; EIMS: *m*/*z* (%, assignment): 847 (1, [M^+]), 697 (1, [M^+–CF_3SO_3]), 604 (8), 455 (34, [M^+–CF_3SO_3–$C_{14}H_{18}N_4$]), 329 (2), 325 (6), 266 (3), 242 (100, [M^+–Zn(CF_3SO_3)$_2$]), 198 (70, [M^+–Zn(CF_3SO_3)$_2$–N(CH_3)$_2$]), 184 (19), 171 (48), 155 (53), 142 (11, [M^+–Zn(CF_3SO_3)$_2$–C{N(CH_3)$_2$}$_2$]), 128 (14, [M^+–Zn(CF_3SO_3)$_2$–C(N)(N(CH_3)$_2$)$_2$]), 100 (43, [C{N(CH_3)$_2$}$_2$]$^+$); elemental analysis calcd (%) for $C_{30}H_{36}N_8O_6F_6S_2Zn$: C 42.38, H 4.24, N 13.18; found: C 42.41, H 4.54, N 13.14.

General procedure for lactide polymerisation: D,L-Lactide (3.603 g, 25 mmol) and the initiator (I/M ratio 1/500 or 1/1000) were weighed into a 50 mL Erlenmeyer flask, which was closed with a glass stopper. The reaction vessel was then heated at 130 or 150°C. After the reaction time the polymer melt was allowed to cool to room temperature and then dissolved in 25 mL of dichloromethane. The PLA was precipitated in 350 mL of ice-cooled ethanol und dried under vacuum at 50°C.

Acknowledgements

Financial support by the Universität Paderborn (fellowship for S.H.-P.) is gratefully acknowledged. J.B. thanks the Stiftung der Deutschen Wirtschaft for granting a PhD fellowship. Furthermore, S.H.-P. thanks Prof. Dr. G. Henkel for his valuable support.

[1] a) H. R. Kricheldorf, *Chemosphere* **2001**, *43*, 49; b) H. R. Kricheldorf, K. Bornhorst, H. Hachmann-Thiessen, *Macromolecules* **2005**, *38*, 5017; c) H. R. Kricheldorf, S. Rost, *Polymer* **2005**, *46*, 3248; d) H. R. Kricheldorf, H. Hachmann-Thiessen, G. Schwarz, *Biomacromolecules* **2004**, *5*, 492.

[2] J. Wu, T.-L. Yu, C.-T. Chen, C.-C. Lin, *Coord. Chem. Rev.* **2006**, *250*, 602.

[3] B. J. O'Kneefe, M. A. Hillmyer, W. B. Tolman, *Dalton Trans.* **2001**, 2215.

[4] R. W. Drumwright, P. R. Gruber, D. E. Henton, *Adv. Mater.* **2000**, 12, 1841.

[5] R. Mehta, V. Kumar, H. Bhunia, N. S. Upadhyay, *J. Macromol. Sci. Polym. Rev.* **2005**, *45*, 325.

[6] O. Dechy-Cabaret, B. Martin-Vaca, D. Bourissou, *Chem. Rev.* **2004**, *104*, 6147.

[7] D. Garlotta, *J. Polym. Environ.* **2001**, *9*, 63.

[8] K. Nakano, N. Kosaka, T. Hiyama, K. Nozaki, *Dalton Trans.* **2003**, 4039.

[9] M. Okada, *Prog. Polym. Sci.* **2002**, *27*, 87.

[10] S. Jacobsen, P. Degée, H. G. Fritz, P. Dubois, R. Jérôme, *Polym. Eng. Sci.* **1999**, *39*, 1311.

[11] R. Mazarro, A. de Lucas, I. Gracia, J. F. Rodríguez, *J. Biomed. Mater. Res. Part B* **2007**, *85*, 196.

[12] M. Cheng, A. B. Attygalle, E. B. Lobkovsky, G. W. Coates, *J. Am. Chem. Soc.* **1999**, *121*, 11583.

[13] B. M. Chamberlain, M. Cheng, D. R. Moore, T. M. Ovitt, E. B. Lobkovsky, G. W. Coates, *J. Am. Chem. Soc.* **2001**, *123*, 3229.

[14] M. H. Chisholm, J. C. Gallucci, H. S. Zhen, *Inorg. Chem.* **2001**, *40*, 5051.

[15] S. C. Cole, M. P. Coles, P. B. Hitchcock, *Organometallics* **2004**, *23*, 5159.

[16] A. P. Gupta, V. Kumar, *Eur. Polym. J.* **2007**, *43*, 4053.

[17] J. Börner, S. Herres-Pawlis, U. Flörke, K. Huber, *Eur. J. Inorg. Chem.* **2007**, 5645.

[18] a) H. Wittmann, A. Schorm, J. Sundermeyer, *Z. Anorg. Allg. Chem.* **2000**, *626*, 1583; b) S. H. Oakley, D. B. Soria, M. P. Coles, P. B. Hitchcock, *Polyhedron* **2006**, *25*, 1247; c) H. Wittmann, V. Raab, A. Schorm, J. Plackmeyer, J. Sundermeyer, *Eur. J. Inorg. Chem.* **2001**, 1937; d) S. Aoki, K. Iwaida, N. Hanamoto, M. Shiro, E. Kimura, *J. Am. Chem. Soc.* **2002**, *124*, 5256; e) T. Ishikawa, M. Kawahata, EP 1752451A1, **2007**.

[19] a) U. Köhn, M. Schulz, H. Görls, E. Anders, *Tetrahedron: Asymmetry* **2005**, *16*, 2125; b) M. Walther, K. Wermann, M. Lutsche, W. Günther, H. Görls, E. Anders, *J. Org. Chem.* **2006**, *71*, 1399.

[20] M. Coles, P. Hitchcock, *Eur. J. Inorg. Chem.* **2004**, 2662.

[21] N. Ajellal, D. M. Lyubov, M. A. Sinenkov, G. K. Fukin, A. V. Cherkasov, C. M. Thomas, J.-F. Carpentier, A. A. Trifonov, *Chem. Eur. J.* **2008**, *14*, 5440.

[22] N. Kuhn, M. Grathwohl, M. Steimann, G. Henkel, *Z. Naturforsch.* **1998**, *53b*, 997.

[23] a) M. Tamm, D. Petrovic, S. Randoll, S. Beer, T. Bannenberg, P. G. Jones, J. Grunenberg, *Org. Biomol. Chem.* **2007**, *5*, 523; b) D. Petrovic, L. M. R. Hill, P. G. Jones, W. B. Tolman, M. Tamm, *Dalton Trans.* **2008**, 887; c) T. K. Panda, C. G. Hrib, P. G. Jones, J. Jenter, P. W. Roesky, M. Tamm, *Eur. J. Inorg. Chem.* **2008**, 4270.

[24] S. Herres-Pawlis, U. Flörke, G. Henkel, *Eur. J. Inorg. Chem.* **2005**, 3815.
[25] S. Herres-Pawlis, A. Neuba, O. Seewald, T. Seshadri, H. Egold, U. Flörke, G. Henkel, *Eur. J. Org. Chem.* **2005**, 4879.
[26] A. Hoffmann, J. Börner, U. Flörke, S. Herres-Pawlis, *Inorg. Chim. Acta*, **2008**, DOI: 10.1016/j.ica.2008.06.002.
[27] M. A. Khan, D. G. Tuck, *Acta Crystallogr. Sect. C* **1984**, *40*, 60.
[28] C. W. Reimann, S. Block, A. Perloff, *Inorg. Chem.* **1966**, *5*, 1185.
[29] P. Steel, C. Sumby, *Dalton Trans.* **2003**, 4505.
[30] a) A. Neuba, R. Haase, M. Bernard, U. Flörke, S. Herres-Pawlis, *Z. Anorg. Allg. Chem.* **2008**, *634*, 2511; b) V. Raab, Ph.D. Thesis, University of Marburg, **2001**; c) S. Herres-Pawlis, Ph.D. Thesis, University of Paderborn, **2005**.
[31] Gaussian 03, Revision C.01, M. J. Frisch, G. W. Trucks, H. B. Schlegel, G. E. Scuseria, M. A. Robb, J. R. Cheeseman, J. A. Montgomery, Jr., T. Vreven, K. N. Kudin, J. C. Burant, J. M. Millam, S. S. Iyengar, J. Tomasi, V. Barone, B. Mennucci, M. Cossi, G. Scalmani, N. Rega, G. A. Petersson, H. Nakatsuji, M. Hada, M. Ehara, K. Toyota, R. Fukuda, J. Hasegawa, M. Ishida, T. Nakajima, Y. Honda, O. Kitao, H. Nakai, M. Klene, X. Li, J. E. Knox, H. P. Hratchian, J. B. Cross, C. Adamo, J. Jaramillo, R. Gomperts, R. E. Stratmann, O. Yazyev, A. J. Austin, R. Cammi, C. Pomelli, J. W. Ochterski, P. Y. Ayala, K. Morokuma, G. A. Voth, P. Salvador, J. J. Dannenberg, V. G. Zakrzewski, S. Dapprich, A. D. Daniels, M. C. Strain, O. Farkas, D. K. Malick, A. D. Rabuck, K. Raghavachari, J. B. Foresman, J. V. Ortiz, Q. Cui, A. G. Baboul, S. Clifford, J. Cioslowski, B. B. Stefanov, G. Liu, A. Liashenko, P. Piskorz, I. Komaromi, R. L. Martin, D. J. Fox, T. Keith, M. A. Al-Laham, C. Y. Peng, A. Nanayakkara, M. Challacombe, P. M. W. Gill, B. Johnson, W. Chen, M. W. Wong, C. Gonzalez, and J. A. Pople, Gaussian, Inc., Wallingford CT, **2004**.
[32] G. Frison, G. Ohanessian, *J. Comput. Chem.* **2007**, *28*, 416.
[33] S. Wörl, D. Hellwinkel, H. Pritzkow, M. Hofmann, R. Krämer, *Dalton Trans.* **2004**, 2750.
[34] S. Herres, U. Flörke, G. Henkel, *Acta Crystallogr. Sect. C* **2004**, *60*, o358–o360.
[35] V. Raab, J. Kipke, R. M. Gschwind, J. Sundermeyer, *Chem. Eur. J.* **2002**, *8*, 1682.
[36] a) G. Schwach, J. Coudane, R. Engel, M. Vert, *Polym. Bull.* **1994**, *32*, 617; b) M. H. Chisholm, J. C. Galluci, H. Yin, *Proc. Natl. Acad. Sci. USA* **2006**, *103*, 15315.
[37] a) B. G. G. Lohmeijer, R. C. Pratt, F. Leibfarth, J. W. Logan, D. A. Long, A. P. Dove, F. Nederberg, J. Choi, C. Wade, R. M. Waymouth, J. L. Hedrick, *Macromolecules* **2006**, *39*, 8574; b) R. C. Pratt, B. G. G. Lohmeijer, D. A. Long, R. M. Waymouth, J. L. Hedrick, *J. Am. Chem. Soc.* **2006**, *128*, 4556; c) A. Chuma, H. W. Horn, W. C. Swope, R. C. Pratt, L. Zhang, B. G. G. Lohmeijer, C. G. Wade, R. M. Waymouth, J. L. Hedrick, J. E. Rice, *J. Am. Chem. Soc.* **2008**, *130*, 6749.
[38] M. Rubinstein, R. H. Colby in *Polymer Physics*, Oxford University Press, Oxford, **2003**, Chapter 1.
[39] a) G. Rafler, J. Dahlmann, K. Wiener, *Acta Polym.* **1990**, *41*, 328; b) A. Schindler, D. Harper, *J. Polymer Sci. Polymer Chem. Ed.* **1979**, *17*, 2593.
[40] K. Stott, J. Keeler, Q. N. Van, A. J. Shaka, *J. Magn. Reson.* **1997**, *125*, 302.
[41] Bruker, SMART (Version 5.62), SAINT (Version 6.02), SHELXTL (Version 6.10) and SADABS (Version 2.03). Bruker AXS Inc., Madison, Wisconsin, **2002**.
[42] a) A. D. Becke, *J. Chem. Phys.* **1993**, *98*, 5648; b) C. Lee, W. Yang, R. G. Parr, *Phys. Rev. B* **1988**, *37*, 785; c) B. Miehlich, A. Savin, H. Stoll, H. Preuss, *Chem. Phys. Lett.* **1989**, *157*, 200.
[43] *Polymer Data Handbook* (Ed.: J. E. Mark), Oxford University Press, Oxford, **1999**.

Received: October 14, 2008
Published online: January 21, 2009

